Tests to Determine the Behaviour of Riveted Joints of Steel Structures under Alternate Bending Moments.

By Rio Tanabashi.

Assist. Prof. of Architectural Engineering, Kyoto Imperial University, Kyoto, Japan.

I. Introducton.

1. Object of the Tests.

The object of these tests was to determine the behaviour of riveted joints connecting the columns and girders of steel structures under alternate bending moments. The excelent eathquake-proof quality of steel structures was demonstrated in the great disaster that befell the Kwantō Districts in 1923. But this earthquake-proof quality of steel structures has never been investigated either theoretically or experimentally. The present investigations have been carried out in order to ascertain both experimentally and theoretically what these characteristics are.

I may mention that the supreme earthquake-proof quality of steel structures is due primarily the fact that they can stand great deformation without being involved in sudden fatal destruction.

Buildings made of such brittle materials as brick or stone were found to be most dangerous at the time of the earthquake, for they can stand very little deformation and crashed suddenly. On the contrary almost no steel structures were irreparably destroyed by the earthquake shocks, although some of them had been built with no particular attention to the matter of earthquakes.

The reason for this is the superior ductility of iron and steel, which will bear a great strain before finally crashing or pulling out.

The external force acting upon structures in the case of earthquake shocks is remarkably large, but it does not continue for any great length of time. The force acts upon the structures instantaneously and alternately, with the result that the structures vibrate.

But when some part of the steel structure undergoes plastic deformation, the period of vibration is prolonged and effective damping forces occur within the structure that permit no resonance, no violent vibration to bring about the fatal destruction of the structure in question.

It was therefore one of the purposes of the presents tests to study the properties of vibration damping of riveted joints. For this reason, in my research the most ordinary types of connection have been tested under an alternate bending moment far greater than the working load and causes some parts of the joints to strain over the elastic limits.

2. Acknowledgements.

The tests described in this report were made under the aids of the Gwakujutsu Shinkōkwai. Y. Takahashi, Graduate Student in the Architecture Department; J. Dazai, Graduate Stunent in the Architecture Department; M. Itomi, Research Fellow in Architectural Engineering, and E. Yoshimura Assistant of the Architecture Department renderd valuable services by assisting with the tests and the calculations.

II. Description of the tests.

3. Description of the test pieces.

The test pieces are shown in figs. 1 to 9, inclusive. Two pieces of each type were used, each piece having a similar connection of the two sides with the centre column piece.

In selecting the test pieces I aimed at using types of connection common in engineering structures and which resist shears and moments in different ways. Test pieces No. 1, No. 2, and No. 3 are types of cannection primarily designed to resist shear, not moment. Among them, No. 2 is a rather peculiar cannection seldom used. In these types ordinary I-beams are used as girders. No. 4 and No. 5 are types designed to resist both shear and moment and commonly used in Genmany with an H-coupé connecting H-girder, when the

Fig. 1.

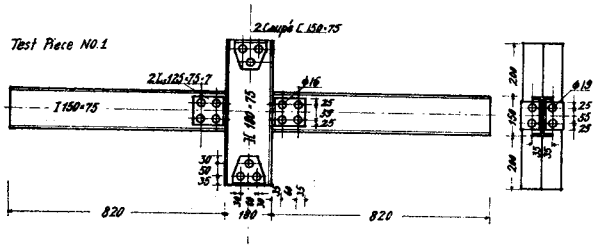

Fig. 2.

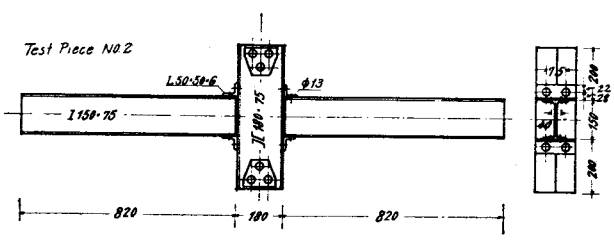

Fig. 3.

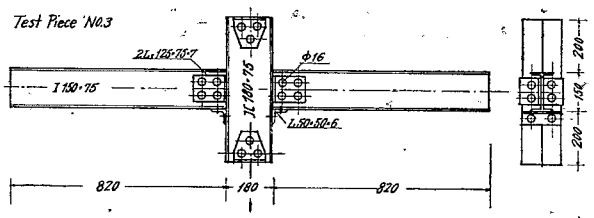

Fig. 4.

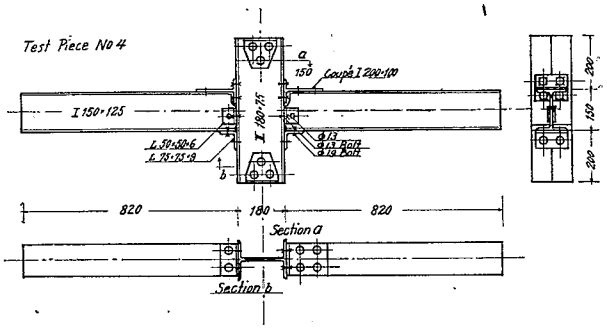

Fig. 5.

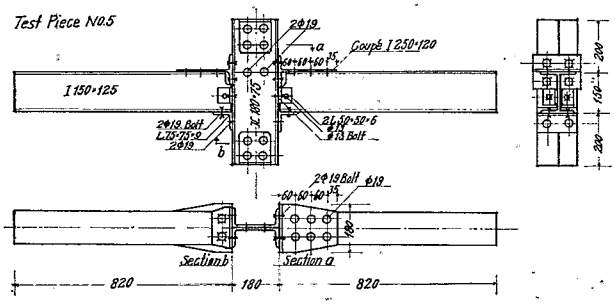

Fig. 6.

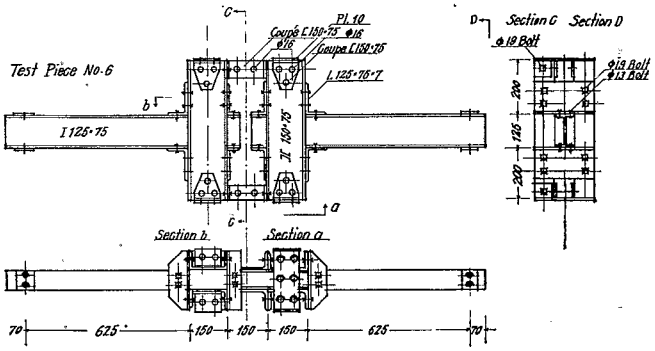

Fig. 7.

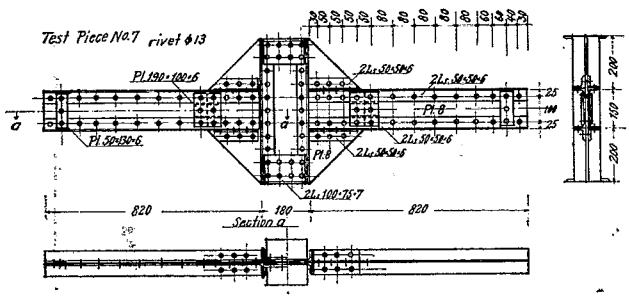

Fig. 8.

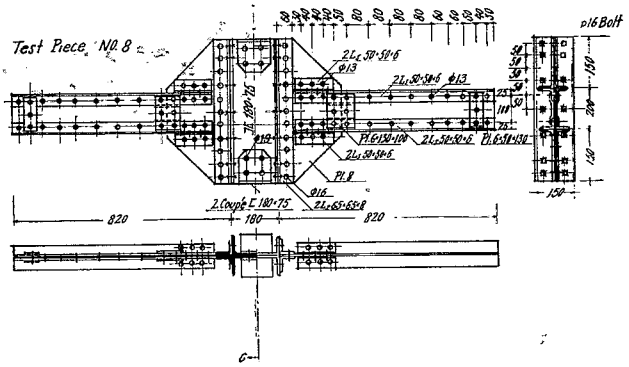

Fig. 9.

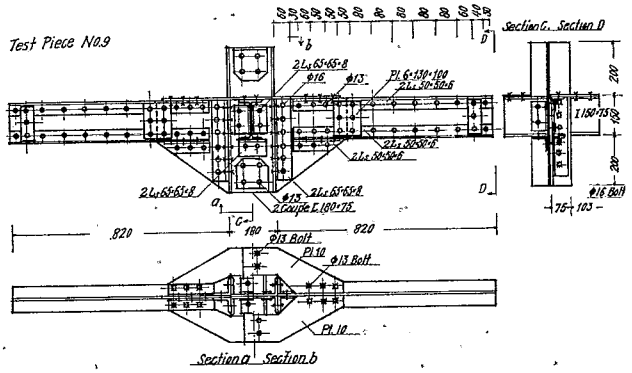

Fig. 10.

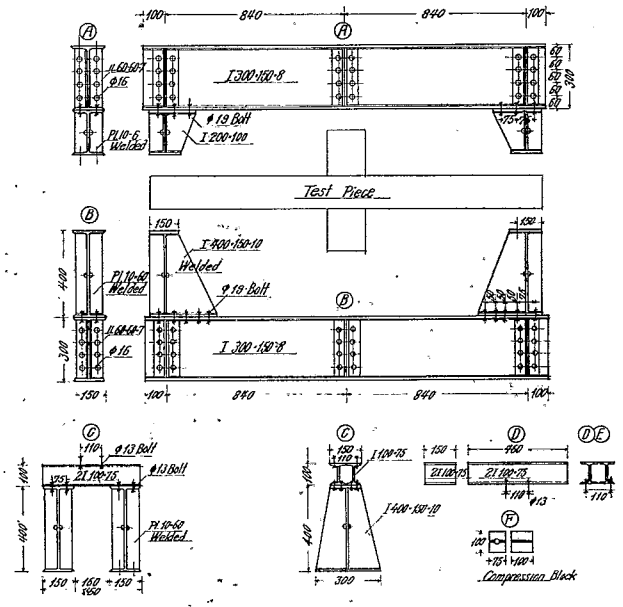

Loading and Supporting Apparatus

Fig. 11.

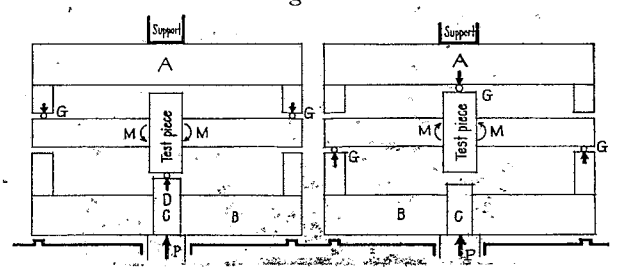

P is the hydraulic driven head of the testing machine.

Fig. 12.

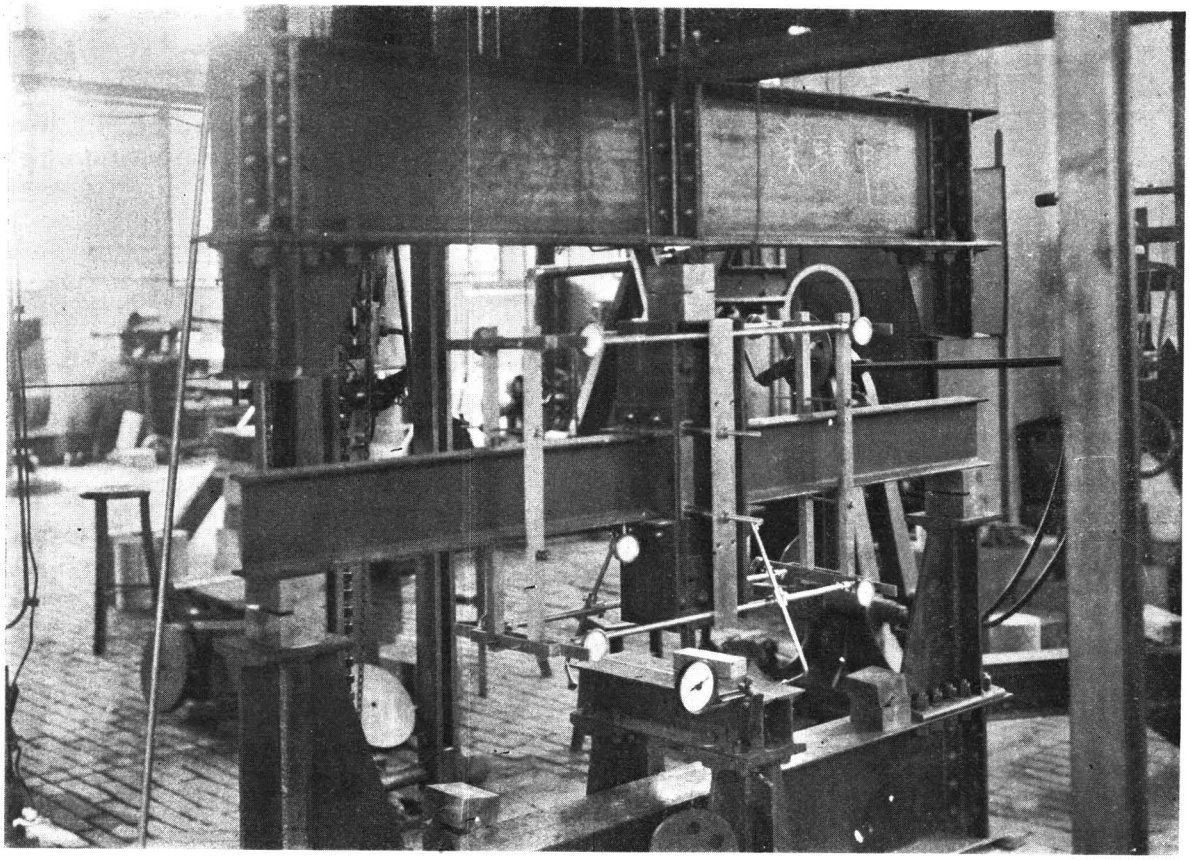

Fig. 13.

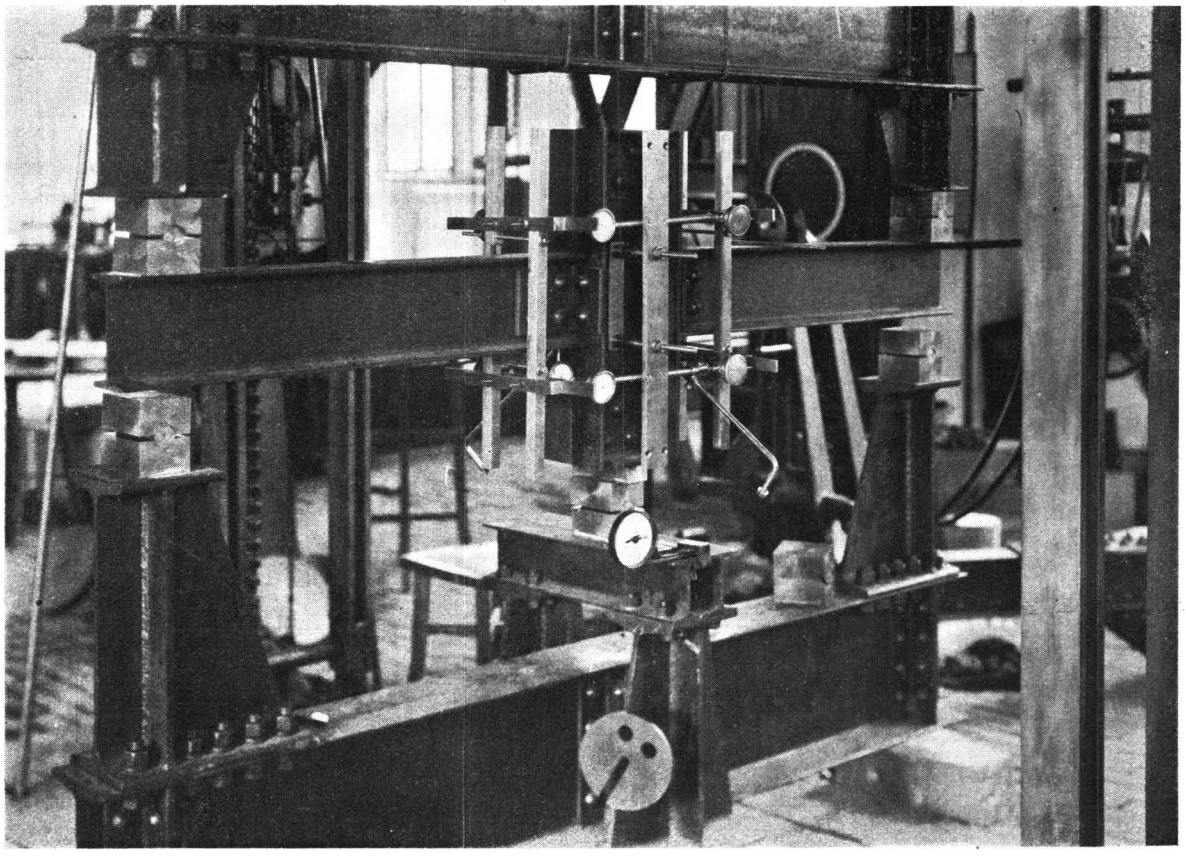

Fig. 14.

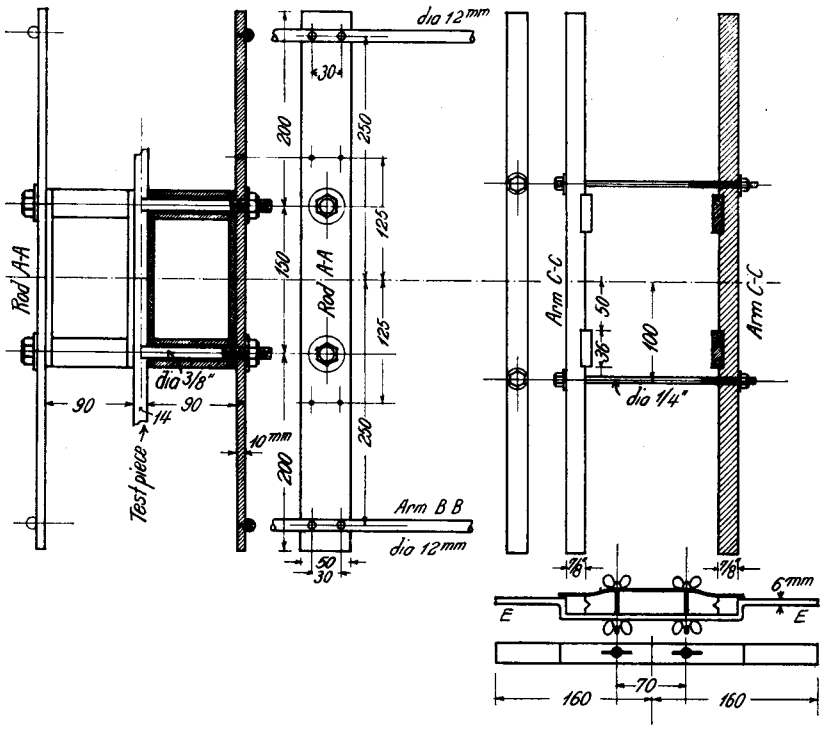

Fig. 15.

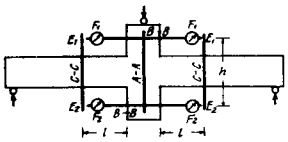

Arrangement for Measuring the Change of Slope.

moment is comparatively large and the girders are of H-section. This type of connection is seldom used in our country. No. 6 is the type of connection, also commonly used in Germany as the most effective rigid joint, but seldom used in our country. No. 7, No. 8, and No. 9 are commonly used types of connection when the girders are composite plate-girders. These types are commonly used in Japan as connections designed to resist both large shear and bending moment, No. 4, No. 5, and No. 9 are specially designed as joints in which the large moment that compresses the top plate is not to be resisted.

The rivets were driven in the shop by means of a press riveter. Black bolts were used in several places instead of rivets.

All these test pieces were manufactured by the Yokokawa Kyōryō Seisakusho of Osaka. They received no more attention than any of the ordinary run of commercial work passing through the shop.

4. *Apparatus and Methods of Testing.*

The test pieces described were tested in a 50,000 kg. Amsler pipe-testing machine. For alternating loading special apparatus was designed as shown in fig. 10.

The alternate loading arrangements are shown schematically in fig. 11. Fig. 12, and fig. 13 are reproductions of photographs of test pieces in the machine in two different ways of loading.

The load is applied at the top and at the bottom of the column alternately, so that the connections of the girders are alternately exposed to positive and negative moments.

At the loading place and the supporting places pins are inserted to permit free rotation of the end of the beam.

The deformation measurements include the rotation of the girder relative to the column, the slip of rivets and the total deflection of the middle point of the test piece.

The measuring apparatus and the arrangement for the change of slope are shown in fig. 14 and fig. 15.

The rod *A-A* is fixed to the axis of the column with bolts and pipe fittings as shown in fig. 15, and two arms *B-B* to which Ames dial-gauges are tightly attached, are also fixed to the rod *A-A*. The position of the arms *B-B* can be changed according to the extent of the change of slope. The rodds are made of two kinds, the one long, the other short. A pair of arms *C-C* with knife-edges are tightly attached to the flanges of the girder by means of two screwed bolts *D*.

If no ratation of the arm *C-C* with respect to the axis of the column takes place, the points *E* adn *F* remain a constant distance apart, but if

rotation does take place, the change of distance between E and F will be a measure of the rotation. If the magnitudes of the changes of distance are denoted by $\triangle S_1$ and $\triangle S_2$ according to the points E_1-F_1 and E_2-F_2, the angle of rotation by θ, the distance between E_1 and E_2 by h, then

$$\tan\theta=(\triangle S_1+\triangle S_2)/h$$

The motion of E with respect to F was measured by means of Ames dial-gauge attached at F. This dial-gauge has a moving range of about 7.5 mm.

The deflection of the test piece, the slip of the rivets at the place of connection in concequence of shearing force, and other small deformations were measured by means of an attached micrometer dial-gauge. Figs. 12 and 13 show the location of the instruments for measurming the deformation of the test pieces.

But all measurement other than the anguler strain are omitted in this report, for the value of the deflections have not yet been accurately determined, and the slips due to shear are different in every case and show no common characteristics permitting a comparison.

III. Discussion of the Results.

5. General Discussion.

In analyzing the stresses in a stiff structure we assume that the connections are perfectly rigid. This assumption means that if tangents are drawn to the elastic curves of two intersecting members at the point where the curves intersect, these tangents do not rotate each other when the connection receives stresses.

The analysis of the stresses in a stiff structure depends upon this assumptien of the perfect rigidity of the connection.

The rigidity of various types of connection has already been studied by Wilbur M. Wilson and Herbert F. Moore of the Engineering Experiment Station of the University of Illinois. They reached the following conclusion.

If the action in the case of a load producing stress equal to one and a half times the working stress is taken as the criterion, connections of the heavy type (such as Nos. 7, 8, and 9) can be consideerd as being perfectly rigid, but the connections of the light type (such as Nos. 1, 2, and 3) connot be consideerd to be perfectly rigid.

In our experiment also, this perfect rigidity of the heavy type connection was ascertained, but as far as the light type connection (mentioned above) is concerned, we cannot agree with the conclutions set out in the Illinois Bulletin.

In Wilson and Moore's report, two assumptions for the computation of the relative rotation of the column and girder were set out. One is that the connection is perfectly rigid, and the other that both members maintain a constant cross-section up to the point of the intersection of the elastic curves of the two members. In cases of light type connection as mentioned above, the relative angular strains measured in the tests are far larger than the value computed on the basis of these two assumptions. Therefore Wilson and Moore concluded that such types of connection cannot be considerd as perfectly rigid for the purpose of analyzing the stresses.

But in the author's opinion, the assumption of the perfect rigidity of the connection under the working stresses does not introduce any serious errors into the results. The source of error lies not in the first assumption, but in the second assumption. In the light type connections the connecting part of the column and girder is quite flexible as compared with the girder or column itself. If we assume another cross-section at the connecting part, smaller than the members themselves, such as the flexibility of the connecting part can be represented, then the stresses in the structures with such light type connections can be analyzed on the assumption of perfect rigidity.

But at the same time it must be mentioned that it is very difficult to represent the flexibility of the connecting part with some smaller cross-section, because the flexibility of the connecting part varies widely with the various types and sizes of connection.

In our experimental study the angular strains are measured up to loads producing some 3 times the working stresses. Under such high loads the rigidity of the connection is almost lost, but the returning curves from such condition are always almost the same as the elastic curves. The characteristics of the hysteresis cycles are explained by models in section 8.

6. Graphic Records.

The test measurements are recorded graphically in graphs 1 to 22.

In these diagrams, measured values are represented by full lines, and computed values by broken lines or chain lines. The distance of the measured point from the end of the girder is given in the graphs as $l=12$ cm. The zero point of the angular strain is indicated by the letters on the upper and lower edges of the graphs for the loop indicated by the same letter. The load-deformation cycles represented as a_1, a_2, b_1, b_2, b_3, b_4, and c_1 etc. mean that the load is so applied succesively, and the beginning of a new letter means that a higher or lower load is applied at first.

The amount of the load applied in such a manner as shown in the right half of fig. 11 is indicated upwards in the graph and the load ap-

plied as shown in the left half of fig. 11 is indicated downwards in the graphs.

The test pieces of type No. 4, No. 5, and No. 9, shown in figs. 4, 5, and 9, are placed upside down at the time of the test.

7. *Computd Strength and Change of Slope of the Test Pieces.*

One of the purposes of our experiment is to determine to what extent the connections calculated and designed to resist bending moment by engineers with light of present knowledge can stand greater bending moment and deformation under alternate loading, that is a similar state to that of earthquake action.

In computing the working load for the test pieces the following unit stresses were used:

Axial bending stress .....1200 kg/cm²
Shear on rivets ..... 800 kg/cm²
Bearing on rivets.....1500 kg/cm²

The computed working loads are given in column 3 of Table 1. The meathods of camputing the working loads on connections of the types used in the tests have not been standardized.

Table 1.

Test. Piece		Weight (kg)	Working load kg.	Maximum Load applied kg.	Safety factor for Maximum load	Manner of Failure
No. 1	A	63,480	±636	± 2,200	2,2~3,8	Connection angle opened
	B	63,910	±(982)	± 2,400		
No. 2	A	60,660	±984	± 3,500	3·5	Lug angle opened
	B	60,450		± 3,500		
No. 3	A	66,030	+984	+ 6,500	6,6	+Lug angle opened
	B	66,840	−982	− 4,000	4,1	−Connection angle opened
No. 4	A	101,500	−4.070	−10,000	2,5~	Web part of Column Channels opened
	B	102,470		+ 4,000		
No. 5	A	105,960	−6,360	−10,000	1,6~	Web part of Column channels opened
	B	107,240		+ 5.000		
No. 6	A	135.7:0	±3,240	± 9,000	2 8	Web of Girder buckled by local compression
	B	134,000				
No. 7	A	93,600	±5,108	±16,000	3,1	Gusset plate yielded
	B	93,800				
No. 8	A	123,200	±5,108	±16,000	3,1	Connection angle opened
	B	123,250				
No. 9	A	126,750	−5,108	±14,000	2,7	+Gusset plate buckled
	B	127,150				−Conection angle opened

In computing the change of slope Young's modulus of structural steel is generaly taken as having the value of 2200 tons per square centimeter. The methods used for computing the change of slope are very different for the various types of connection.

Test Piece No. 1—The strength of the connection for resisting moment can be considerd to be the resistance of four rivets. (see fig. 16) Then the maximum stress upon one rivet will be $4.40 \times P$ (taking P as the load at the end of the girder). The allowable stress upon one rivet is 1.400 tons from the bearing power. So the allowable load upon the middle point of the test piece is 636 kg.

In these calculations we assumed that the edge of the girder is free from stresses. But under certain loads the test piece becomes deformed and the edge of the girder touches the column part. In this condition it is more reasonable to assume that the compressive stress in the flange of the

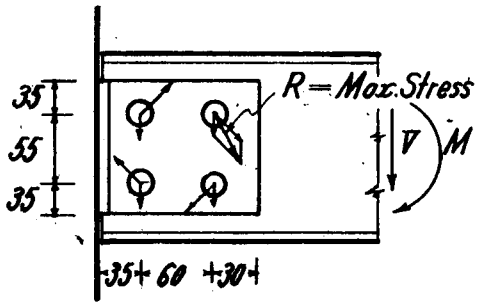

Fig.16

I-girder is directly transmitted to the column. (see fig. 17.) In this case the maximum stress on one rivet is $2.85 \times P$, so that the computed allowable load upon the middle point is 982 kg.

The computation of the change of slope is made as follows:

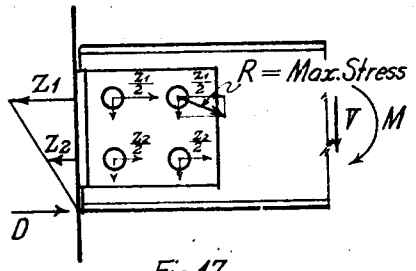

Fig. 17

If we assume that the girder being fixed at the end maintains a constant cross-section, then the extent of the change of slope may be calculated by the following equation.

$$\theta_b=(M_0+M_1)l/2EJ \text{ (see fig. 18),}$$

in which θ_b is the change of slope at the point B,
M_1 is the bending moment at the point B,
M_0 is the bending moment at the fixed end A,
l is the distance between point A and B,
J is the moment of inertia of the girder,
and E is Young's modulus of steel.

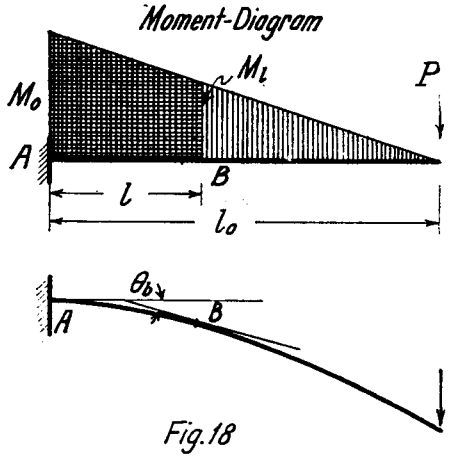

Fig. 18

But in test piece No. 1 we cannot take the constant cross-section for the girder. Because at the end of the girder it is not the girder itself but the connection-angles that resist the bending moment. So that we must assume the moment of inertia of the resisting member as that of the two legs of the connection-angles from some point near the centre of gravity of the group of rivets, which connect the girder and connection-angles, to the fixed end of the girder.

Thus assumed smaller cross-section at the connecting part is not enough to represent the flexibility of the connection, because the most effective part in bringing about the change of slope lies elsewhere. That is the deformation of the connection-angles caused by the bending of the pulled part. (see fig. 19.)

Fig. 19

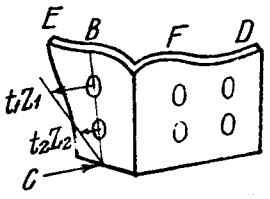

Fig. 20

The deformation of the connection-angles is supposed to be as shown in fig. 20. This deformation is computed approximately in the follwing manner:

The assumption underlying the computation is shown in fig. 21.

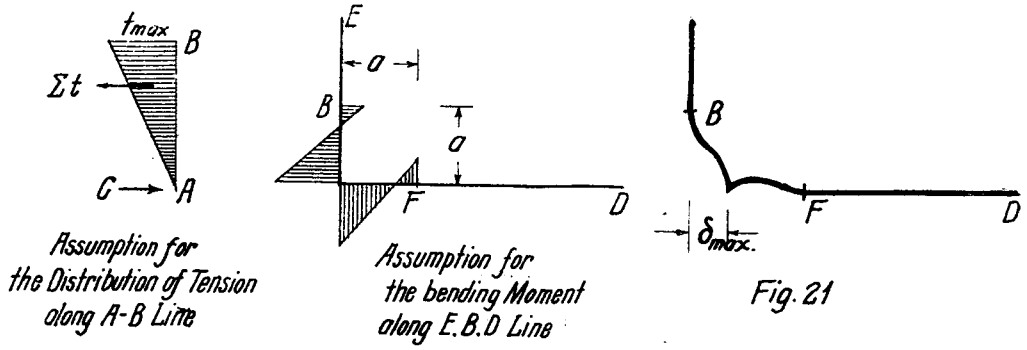

Fig. 21

$$t_{max}=M/\left(10.5^2\times\frac{2}{3}\right)$$

where M is the moment at the connection caused bo load P at the end of the test piece.

$$\delta_{max}=\frac{t_{max}\times a^3}{3EJ}=11.7\times10^{-3}\text{ cm}$$

(for $t_{max}=1$ ton/cm^2)

J=0.0281 cm^4, if the connection-angle having a width of 1 cm and a depth of 0.7 mm considerd to resist to the bending moment.

M for 1 ton load at the middle point is 0.500 $\times 75=37.5$ ton cms. So the t_{max} for a load of 1 ton at the middle point is 0.51 t/cm^2.

Thus computed, the angular strain caused by the bending of connection-angles as shown in fig. 20 is $5{,}78\times10^{-3}$ radians for a load of 1 ton at the middle point of the test piece.

The computed change of slope at the measured point 31 cm from the end of the girder, considering the deformation of the girder and the bending of connection-angles, is 6.91×10^{-3} radians for a load of 1 ton at the middle point of the test piece. Thus computed angular strains are recorded in graphs 1 to 3 by means of chain lines.

If the edge of the girder touches the column, the rotation-axis moves from the edge of the connection-angles to the edge of the girder. In this condition the computed value for the change of slope is 4.55×10^{-3} radians for a load of 1 ton at the middle point. This quantity is recorded in graphs 1 to 3 by means of double chain lines.

The computed quantities are approximately equal to the value experimentally obtained. The flexibility of the light type connection depends upon the type of connection not upon the rigidity of the girder.

At the same time we must notice that with the working load or with slightly higher loads the connection maintains its elastic property approximately.

Test Piece No. 2—The allowable load on the middle point is 984 kg. computed from the allowable shear on rivets 13 mm in diameter. The most effective part for the change of slope is the bending of the lug-angles, which is calculated as follows: (see fig. 22).

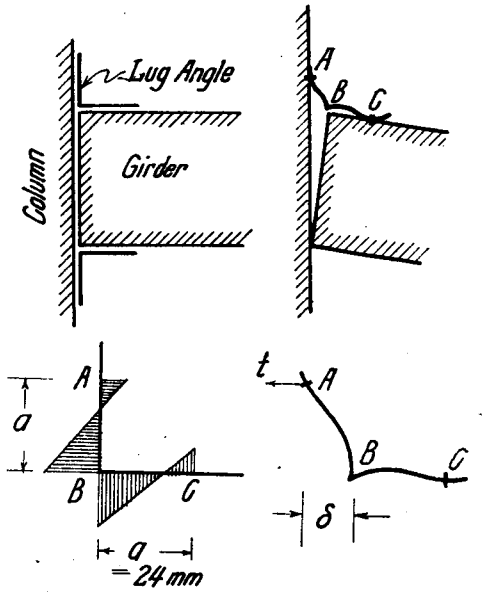

Fig. 22 Assumption for the Distribution of the bending Moment and Deformation

The deflection of the lug-angle of the tension-side of the girder

$$\delta = \frac{t \times a^3}{3EJ} = 7.640 \times 10^{-3} \text{ cm for } t = 1 \text{ ton.}$$

The moment of inertia of the lug-angle for bending is 0.270 cm^4. Thus the angular strain caused by the deformation of the lug-angles is 2.29×10^{-3} radians for a load of 1 ton.

The anguiar strain of the measured point (31 cm from the end of the girder) is 1.79×10^{-3} radians for a load of 1 ton. These quantities are variable with the supposed effective length of a leg of a lug-angle. If we take the effective length of the leg of a lug-angle for bending as being 24+3 mm instead of 24 mm, then the change of slope for a load 1 ton is 2.37×10^{-3} radians.

The first value is recorded in graphs 4 to 7 in chain lines, and the second value is recorded in graph 4 in double chain lines.

These quantities the first and the second, are approximately equal to the quantities obtained by experiment. And this type of connection also maintains its elastic property under the working load or slightly higher loads.

Test Piece No. 3—The allowable load in negative direction is 982 kg, the same load as the second case of the test piece No. 1. Also the change of slope for the negasitive load is computed in the same way as in the second case of the test piece No. 1. The allowable load for the positive direction is considered to be the same as in the case of test piece No. 2. In Computation of the change of slope for the positive direction the bending of the lug-angles and that of the connection-angles are considerd as follows. (see fig. 23).

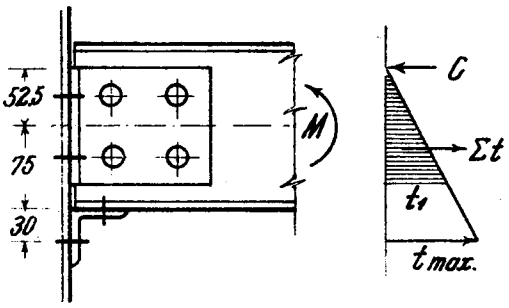

Fig. 23

The angular strain caused by the deformation of a lug angle is $\frac{7.740}{12.76} \times 10^{-3}$ radians for 1 ton of t_{max}.

The angular strain caused by the bending of the connection-angles is $\delta = \frac{118.7}{2 \times 10.5} \times 10^{-3}$ radians per 1 ton/cm^2 of t_1. Thus computed, the angular strain is 1.17×10^{-3} radians for a load of 1 ton at the middle point of the test piece, and the change of slope for the positive load at a point 12 cm from the fixed end of the girder is 1.32×10^{-3} radians, and that of a point 31 cm from the fixed end is 1.62×10^{-3} radians for a load of 1 ton at the middle point of the test piece.

The change of slope for the negative load at the point 12 cm from the end of the girder is 3.57×10^{-3} radians for a load of 1 ton, and the change of slope at the point 31 cm from the end of teh girder is 3.87×10^{-3} radians. In these calculations we assumed that the girder maintains a constant cross-section, which is effective to resists bending moment, to the end of the girder.

But there may be some errors caused by the remarkable decrease in the effective moment of inertia at the end of the girder since the tensile stress transmitted by the connection-rivets from the frange of the girder to the legs of the connection-angles.

Test Piece No. 4—The allowable load at the middle point is computed as being 4.07 tons by the allowble bearing power of the rivets 19 mm in diameter connecting the flange of the I-girder with the coupé of the I-girder.

No computed quantities of angular strain nearly equal to those of the tests could be given by the author, for the most effective cause of the change of slope lies in the bending of the web part of the column, which consists of the web parts of two channels assembled together.

Test Piece No. 5—The allowable load on the middle point of the test piece is computed as being 6.36 tons by the allowable tension of the bolts connecting the coupé of I-girder to the column.

For this type of connection also, no computed change of slope nearly equal to those of the tests could be given by the author. The failure in this case also was the opening of the webs of the channels into each other.

Test piece No. 6—The allowable load on the middle point is computed as being 3.24 tons from the section modulus of the girder.

The computed change of slope at a point 27 cm from the edge of the column is 1.20×10^{-3} radians for a load of 1 ton, when the girder is considerd to be fixed at the edge of the column. And this becomes 1.645×10^{-3} radians when the girder is considerd to be fixed at the axis of the column. The first quantity is recorded in graphs 14 and 15 in broken lines, and the second quantity in chain lines. The latter is nearer to that of the tests.

The curves obtained by the experiment are flat in comparison with the computed ones, because the workmanship of this test piece is not so good, this type of connection being uncommon in Japan, and there is some space between the girder and the lower side of the top angles, making it somewhat less rigid. The lines of the computed quantities (recorded in graphs 14 and 15) are nearly parallel to the return curve of the experimentally measured quantities.

Test Piece No. 7, No. 8, and No. 9—The allowable load of test pieces No. 7, and No. 8 is computed as being 5 108 tons from the bearing power of the rivets 13 mm in diameter connecting the girder with the gusset plate.

The changes of slope of these test pieces are computed as the girder maintains a constant cross-section up to the connecting edge of the column and is fixed at that point.

The moment of inertia of the composite girder is 1106.53 cm^4, so that the change of slope at a point 25 cm from the edge of the column is 0.674×10^{-3} radians for a load of 1 ton at the middle point of the test piece.

The computed quantities are recorded in graphs 16 to 19 in broken lines, and are nearly equal to those obtained by measurement. If the fixed point of the girder is supposed to be at the axis of the column (as assumed in Wilson and Moore's report), the change of slope at the measured point will be 0.984×10^{-3} radians, and this quantity is too large to that obtained by measurement.

So in a more accurate analysis of the rectangular frame the assumption in regard to the flexual rigidity of the connection must be that the girder maintains a constant cross-section up to the connecting edge of the column, and that the parts from the connecting edge to the intersection of the axis of two members have no flexibility.

8. *Model Explanation of the Load-Deformation Curve of Riveted Joints under Alternate Loading.*

We obtained some considerably complicated load-deformation cycles under alternate loading in our experimental studies, but the models which are suggested by the author explain the characteristics of these cycles very simply.

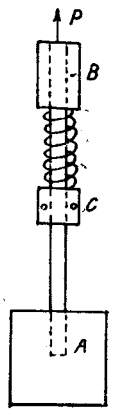

Fig.24

The ordinary hysteresis loop is demonstrated by using a model* shown in fig. 24. It consists of a fixed base A and two movable block B and C which can slide along the rod fixed in A. The block B can slide freely while the block C, attached to B by the helical spring, moves against an adjustable friction. Fig. 25 represents the relation between the force P applied to block B and the desplacement of this block. At a certain load the friction of the block C is overcome and sliding continues without increase in the load.

The ordinary characteristics of the hysteresis loop may be demonstrated with a model consisting of several units simitar to that

* (See Timoshenko, Strength of Materials, P. 680).

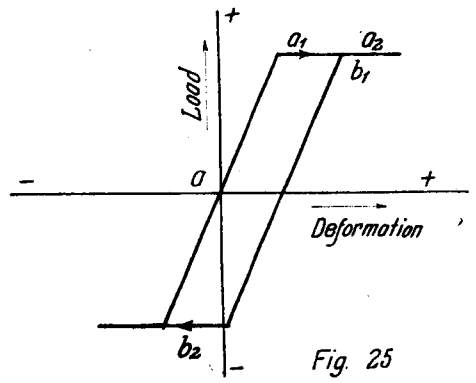

Fig. 25

in fig. 24, put side by side with all block B clamped together. An example of the hysteresis loop obtained by this model is shown in fig. 26.

This type of model is called as the first type by the author.

If we assume that the joint is as one part and the test piece is one complete girder, then the load-deformation curve under alternate loading will be as shown in fig. 26.

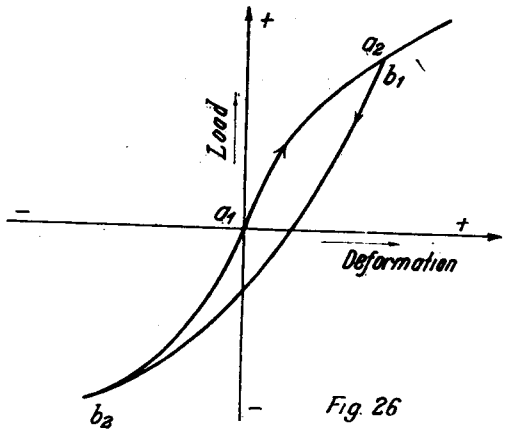

Fig. 26

The characteristics of this loop are as follows:

The curve for an increasing load is always concave to the deformation-axis, whereas the curve for a decreasing load is alwas convex to the deformation-axis, and the curve in the virgin part coinside with the virgin curve, which means that the history has no influence upon the curve in the virgin part, and the return curve b_1-b_2 is made twice as large as the virgin curve a_1-a_2. (see fig. 26.)

These characteristics of the hysteresis loop are demonstrated by Masing's hysteresis model,** and also in my paper "A new model demonstrating the structure and the stress-strain curve of the plastic-elastic material".***

But the cycles obtained by the tests for riveted joints do not show the characteristcs of the first type hysteresis model and appear in quite different shapes.

This is considerd to be caused by the fact that the part subjected to tension and compression under alternate loading making effective deformation is not the part of the complete girder, but the riveted connection.

We may assume that the deformation of a riveted joint can result from a combination of four causes, a) stretch of the plate, b) slip of the plate and rivets, c) compression of the rivets and enlargement of the rivet holes, and d) bending of the rivets.

The causes a) and d) are supposed to possess the property illustrated by fig. 26, whereas the causes b) and c) do not.

For example, in such a case as shown in fig. 27, in which one side of the rivet hole is over compressed and yielded, the permanent set remains when this part is unloaded, which cannot be recoverd by an overload in the opposite direction.

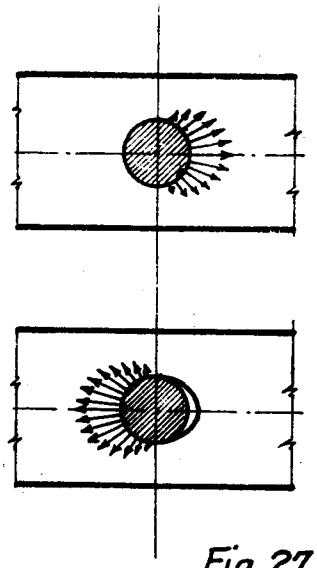

Fig. 27

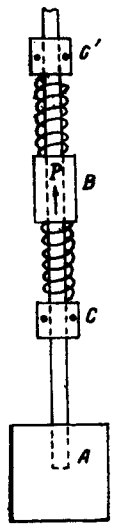

Fig. 28

The rivet may move the full length of the permanent enlargement of the rivet hole under infinitesimal load in the opposite direction.

The ideal load-deformation curve of this part is given in fig. 29, being quite a different shape as compared with fig. 25.

This type of load-deformation curve is demonatrated by the author using a model shown in fig. 28.

It consists of a fixeed base A and three movable block C, C', and B, which can slide along the rod fixed in A. The helical springs are inserted between B and C, and B and C', but they are not fastened to the B block. So the helical springs cannot be pulled, and each of the block C and C' can slide in one direction only.

** G. Masing, Wiss. Veröffi Siemenskonz. 3. 231, 1924.
*** Kenchiku Zasshi, Vol. 46, No. 559, P. 819.

Fig. 29 reprerents the relation between the force P applied to B and the desplacement of this block.

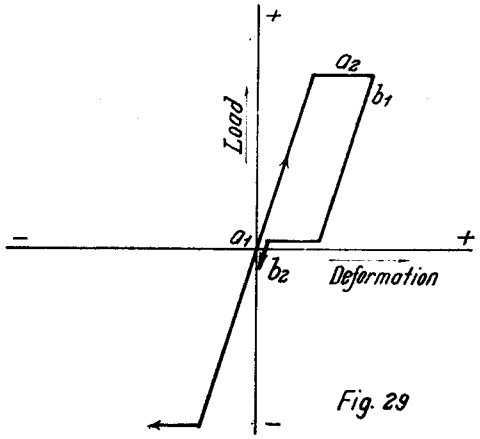

Fig. 29

Generaly the hysteresis loop as shown in fig. 30 may be demonstrated with a model consisting of several units similar to that in fig. 28, put side by side with all blocks B clamped together. This is called the second hysteresis-modell by the author.

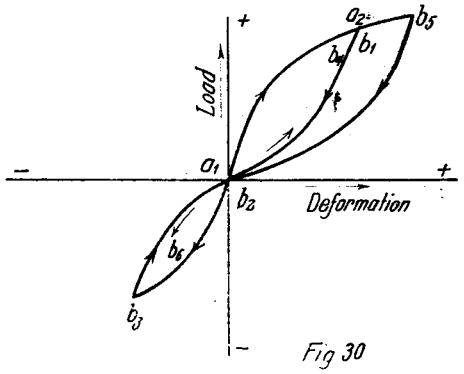

Fig 30

It is considerd to be more reasonable to, assume that the deformation caused by b) and c) follows the cycles indicated by this second hysteresis-model.

The general properties of cycles of the second hysteresis-model are as follows:

The curve in the virgin domain coinside with the virgin curve, and are not affected by its history (this is common with the first hysteresis-model) And the return curve b_1-b_2 is similar to the virgin curve a_1-a_2. And the curves of the repeated load coinside with the return curve from the highest load within the non-virgin domain.

The load-deformation cycles of riveted joints are conveniently demonstrated by a combination of the hysteresis model of the first type and the second type.

The shape of the cycles differs according to the rate of the part that follows the first model and the part that follows the second model, and the shape of the virgin curve of each model. Generally the joints of heavy types are more like the first model, and the joints of light types are more like the second model.

It is supposed in these hysteresis-models that the curve changes suddenly its direction at the passing point from the domain of repeated loads to the virgin domain, which is also experimentally recognized. The sudden change of direction at the O-load when the highest positive and highest negative load in its history are unequal is not clearly observed in experiments.

The cycles of the load-deformation curve obtained theoretically from a combined model are indicated for example, in fig. 31. The combined model of fig. 31 consists of an A-part, for which the first model is taken and B-part, for which the second model is taken, and both parts show the same virgin curve.

Generaly the virgin curves of the A-part and the B-part differ from each other. The virgin

Fig. 31.

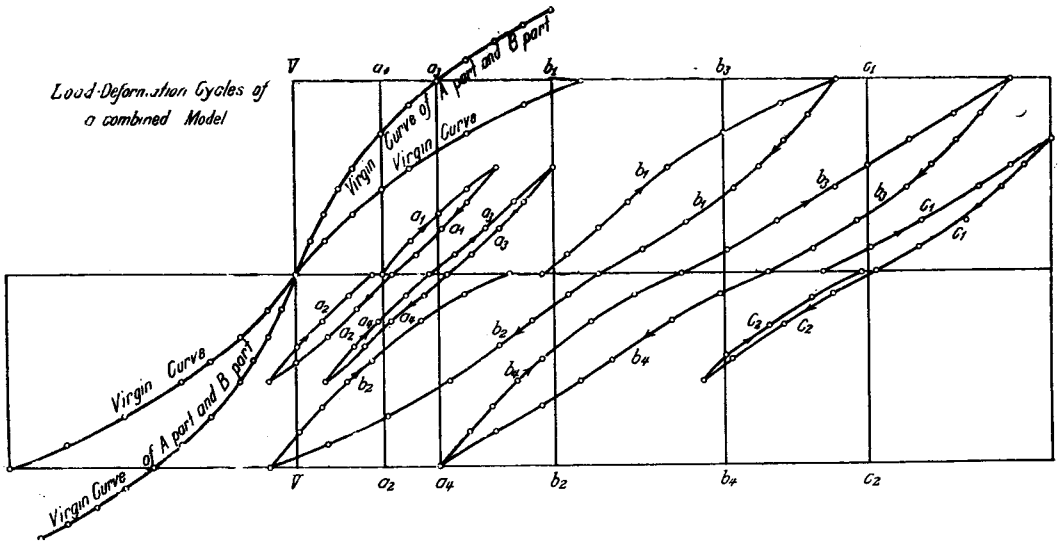

curve of the *A*-part and the *B*-part of the combined model may be determined experimentally from the virgin curve and the return curve from every point on the virgin curve, though in my investigations no quantitative analysis of the cycles was obtained from the virgin curve and return curves in experiments.

But the general characteristics of the load-deformation cycles of riveted joints are clearly demonstrated by the combined model constructed by the author.

And also it must be noticed that not only the load deformation cycles of riveted joint under alternate loading but that of the wooden structures and reinforced concrete structures are quite similar to the cycles of the combined model.

9. *Conclusion.*

The ductilty of rivetded joints is remarkably great, and in these tests, though load some 3 times as large as the working load was applied to each test pieces to bring about very great angular strain, no part of the joint was pulled out or crashed.

In these over-loaded test pieces no visible deformatien remained after smaller load cycles were applied, as would happen in the case of an earthquake.

This characteristic is noteworthy as being one of the superior earthquake-proof qualities of steel structures. Under load higher than the working load the rigidity of joints decreases remarkably, but the load-deformation cycles take in a remarkable area and the consumption of energy shown by this enveloped area of the hysteresis loop acts as a vibration damping source upon the structure. Thus the overbending of structural steel joints under earthquak influence is not in itself dangerous to the stability of the structure, and no effect of resonance is to be feared on the stability of the structure, as the upper limit of the deformation caused by the resonance lies at the elastic limit of the deformaion of the structure, this being quite harmless from the point of view of the safety of the structures.

Though the enveloped area of load-deformation cycles decreases under the second action of load, but the vibration damping quality is not lost. Moreover if another larger shock follows and acts upon the structure, then remarkable energy consumption is accomplished by the overbending of joints, and the amplitude of the vibration decreases rapidly. This is one of the most recommendable earthquake-proof qualities of steel structures that the author can think of.

(Received on January 19, 1935.)

Graph. 1.

Graph. 1 (*An*)

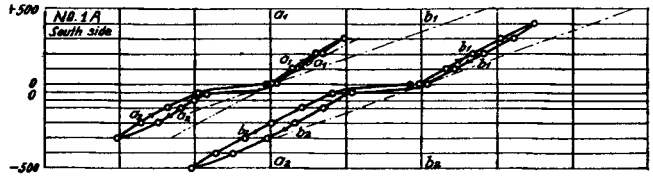

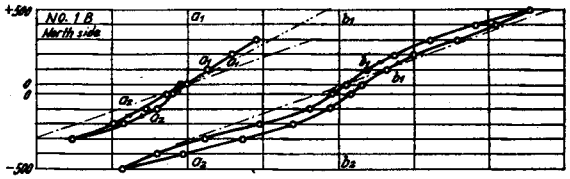

Graph. 1 (*Bn*)

Graph. 1 (*As*)

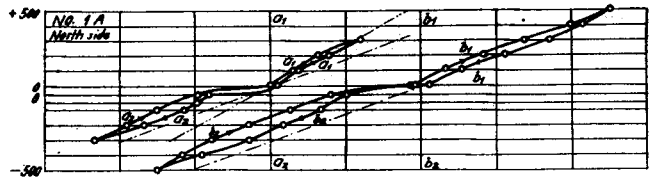

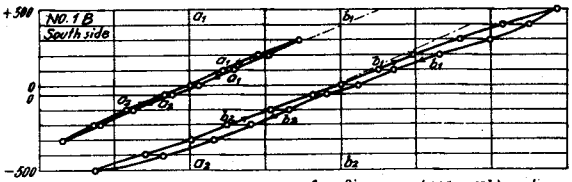

Graph. 1 (*Bs*)

One Division = ($1.25 \cdot 10^{-3}$) radian

Graph. 2.

Graph. 2 (*As*)

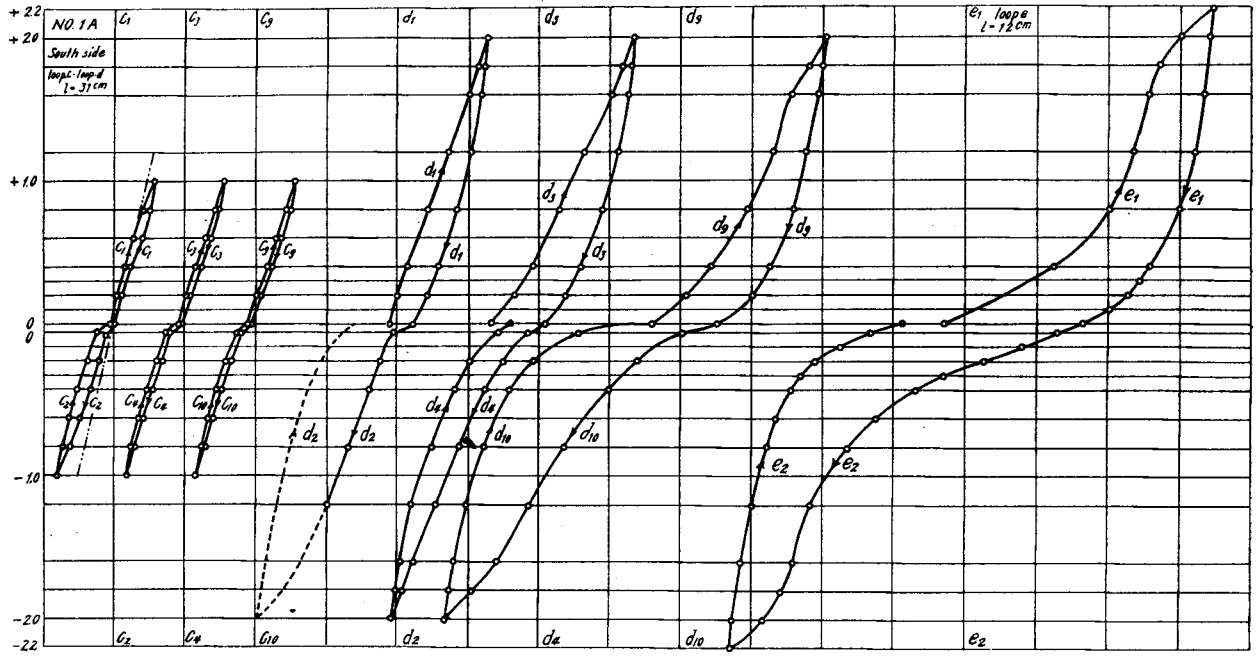

Graph. 2 (*An*)

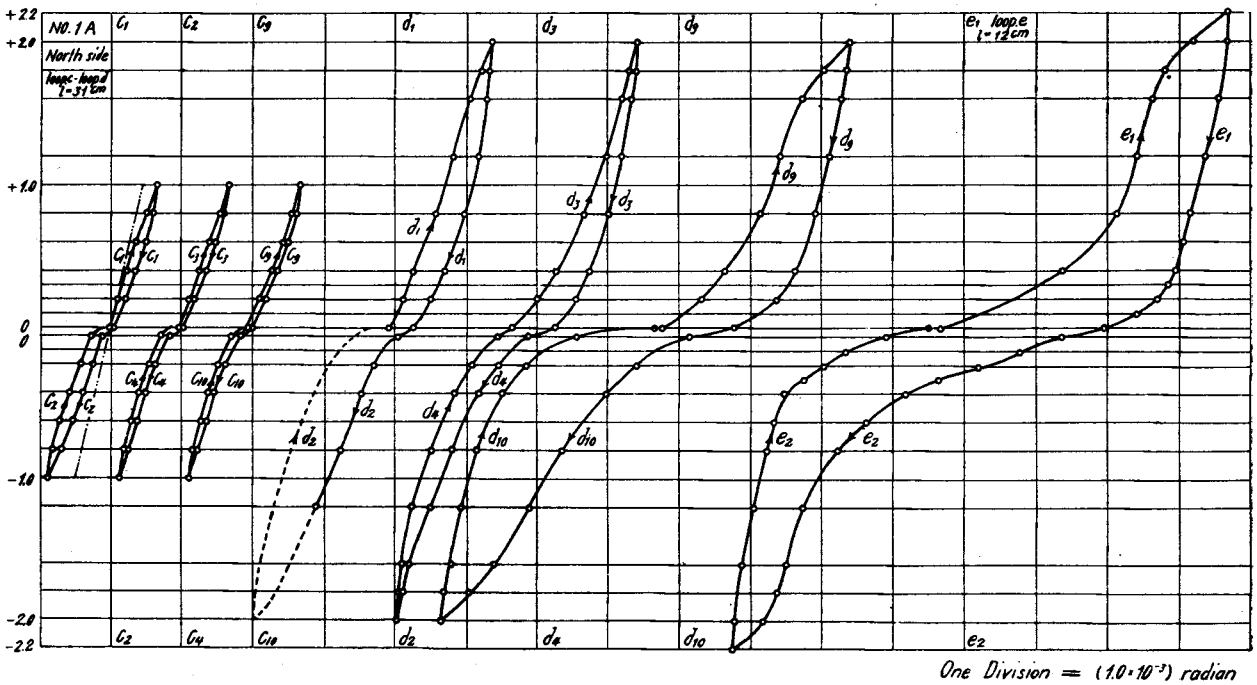

One Division = ($1.0 \cdot 10^{-3}$) radian

Graph. 3.

Graph. 3 (*Bn*)

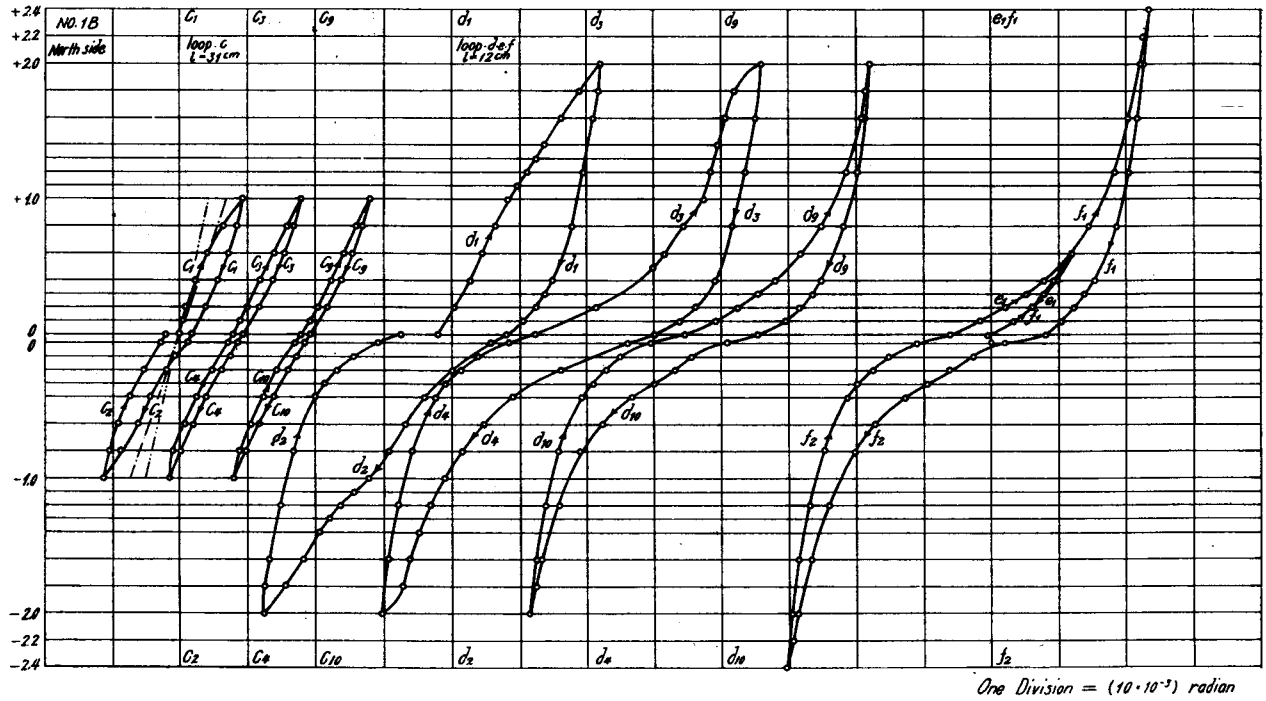

Graph. 3 (*Bs*)

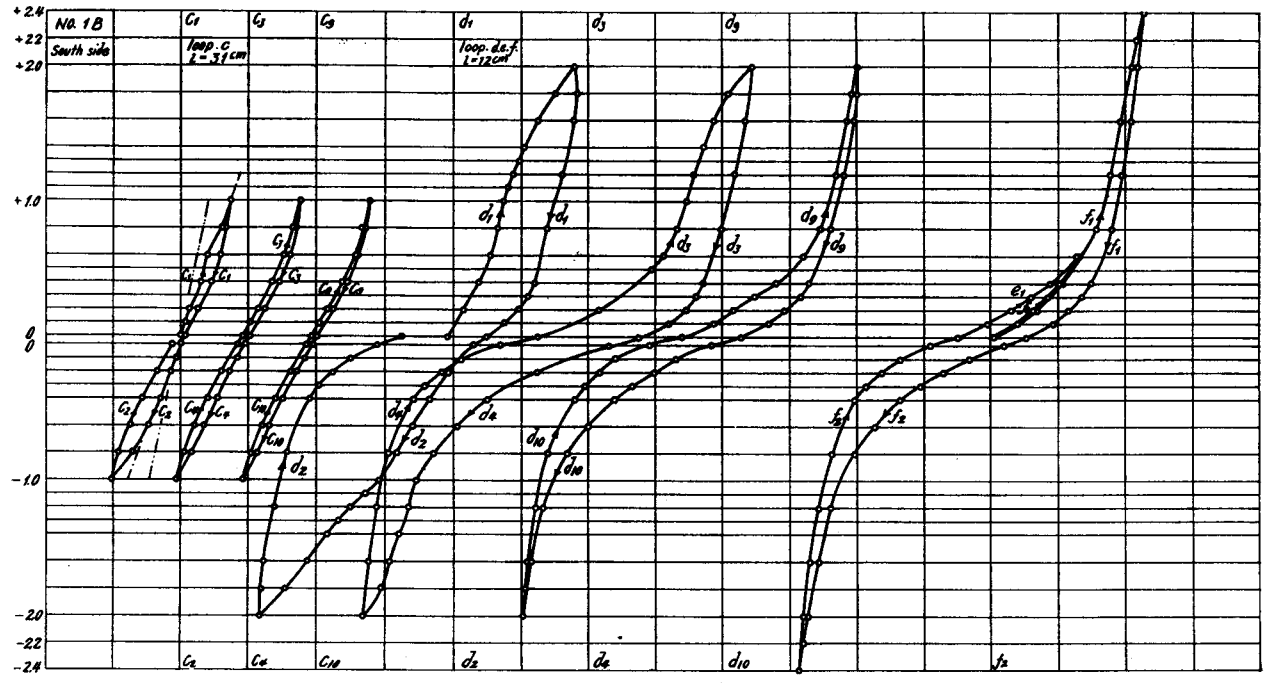

Graphs. 1, 2, 3. Results for Test Piece No. 1.

Graph. 4.

Graph. 4 (*An*)

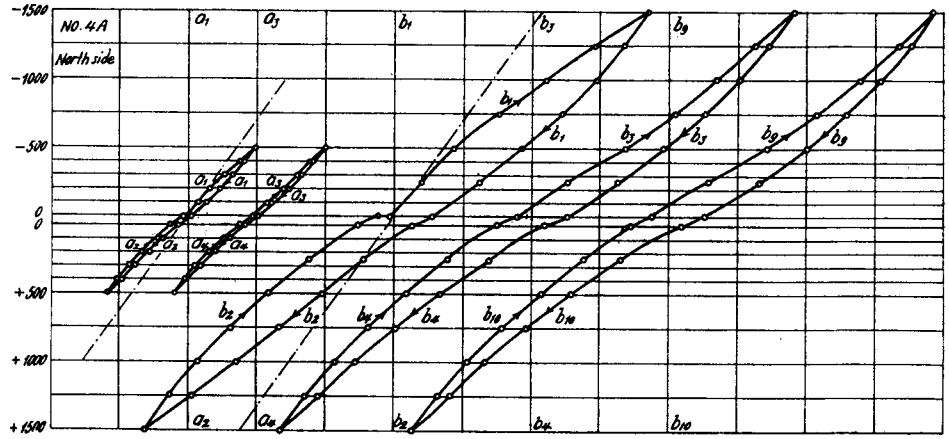

Graph. 4 (*As*)

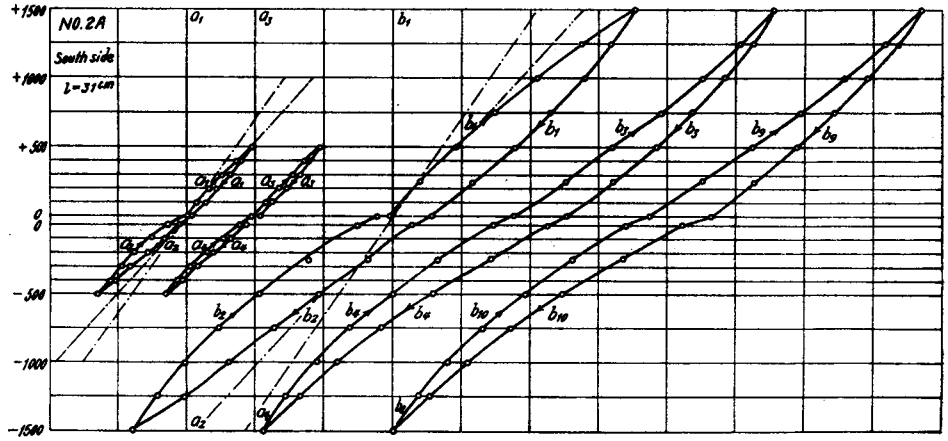

One Dinsion = (125·10⁻³) radian

Graph. 5.

Graph. 5 (*An*)

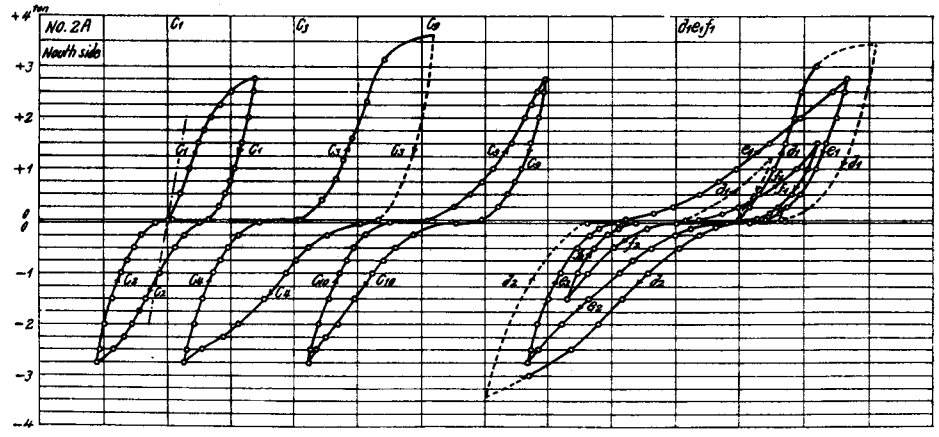

Graph. 5 (*As*)

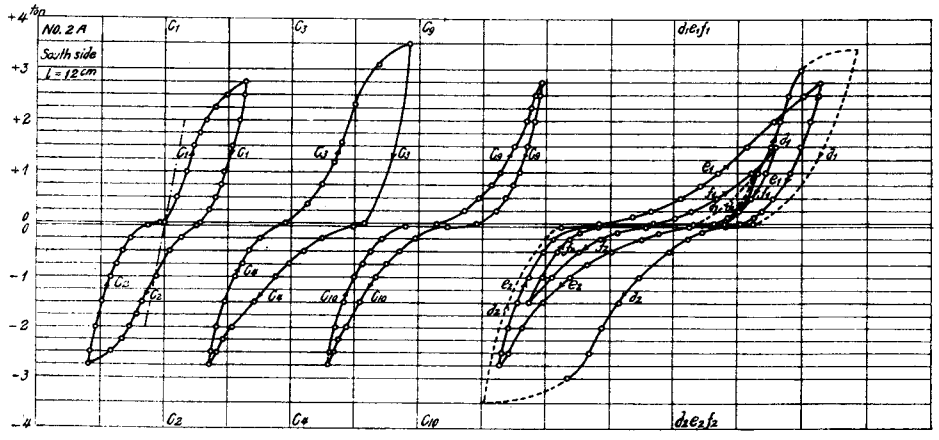

One Division = (10·10⁻³) radian

Graph. 6.

Graph. 6 (*Bn*)

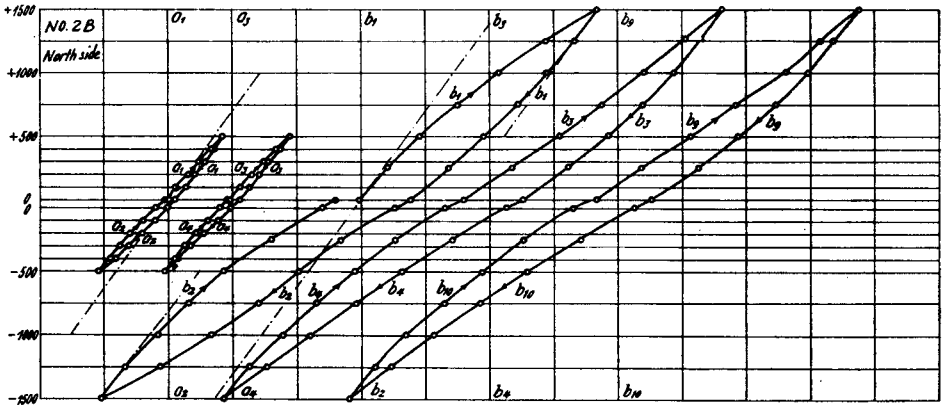

Graph. 6 (*Bs*)

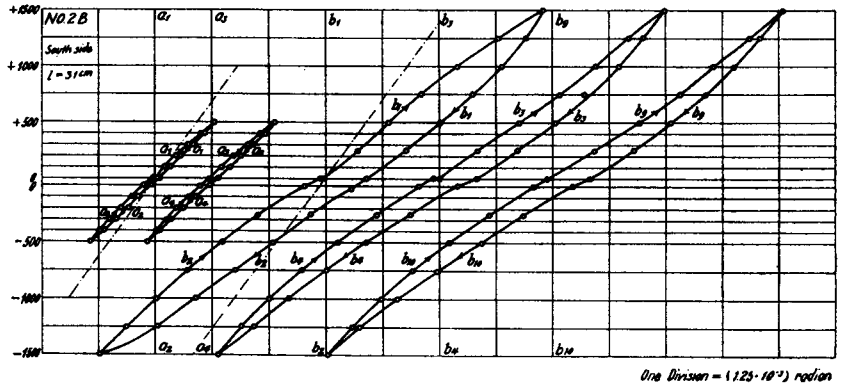

Graph. 7.

Graph. 7 (*Bn*)

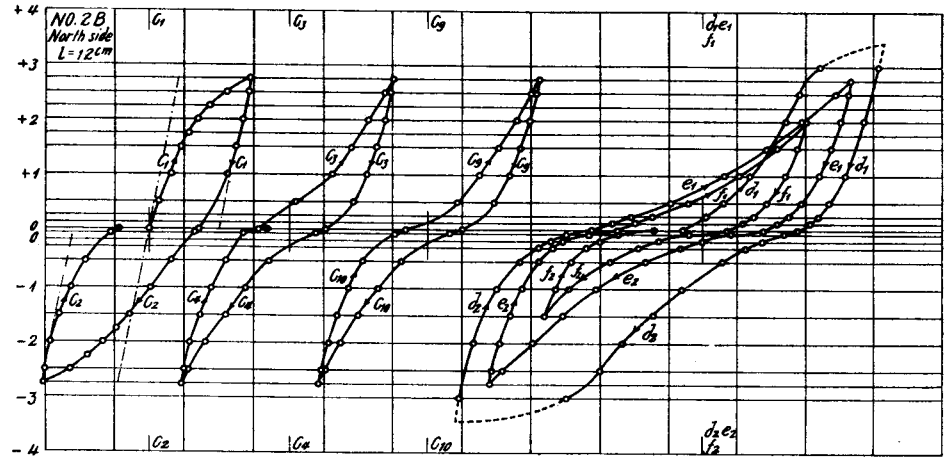

Graph. 7 (*Bs*)

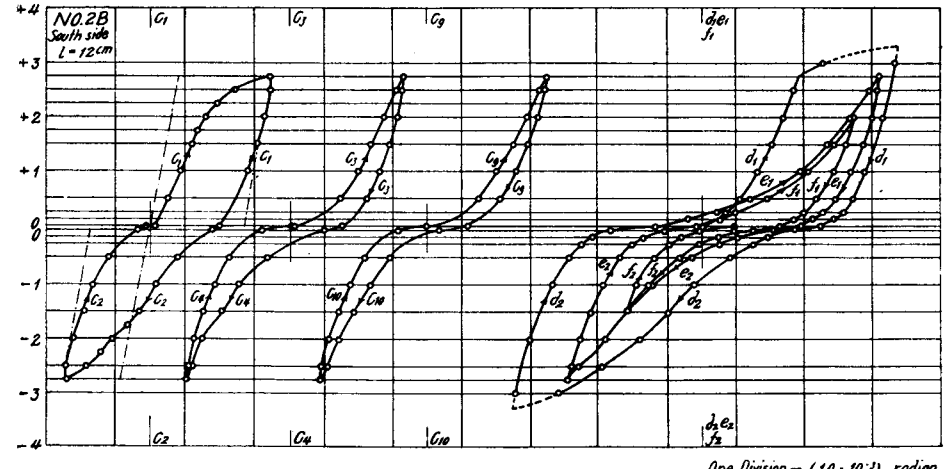

Graphs. 4, 5, 6, 7. Results for Test Piece No. 2.

Graph. 8.

Graph. 8 (*As*)

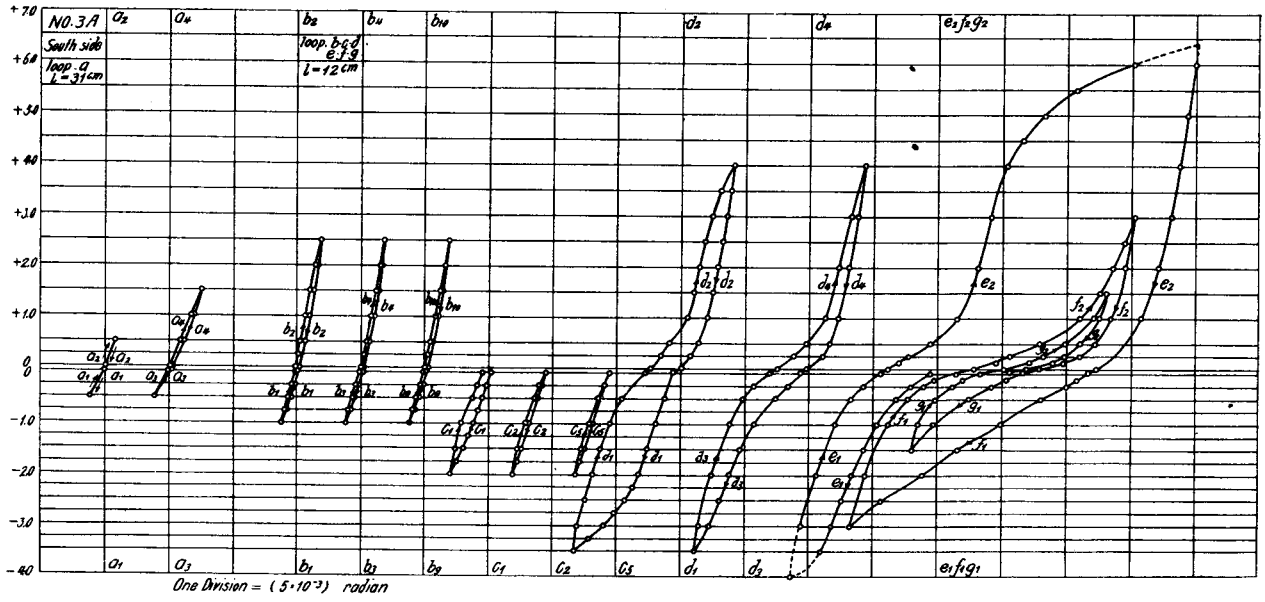

Graph. 8 (*An*)

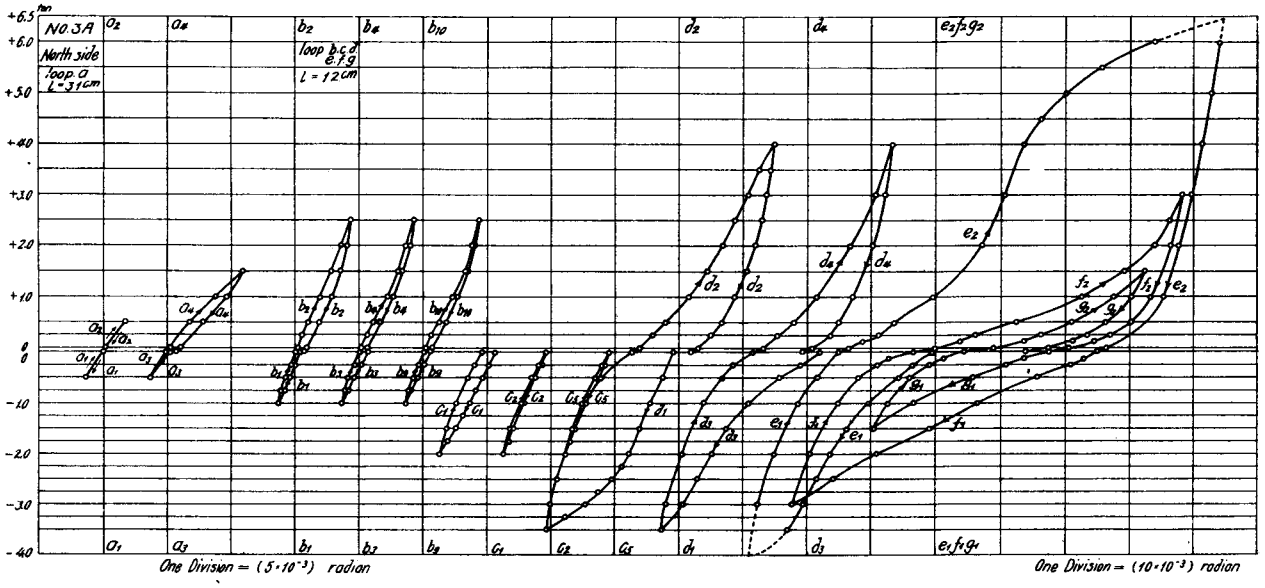

Graph. 9.

Graph. 9 (*Bn*)

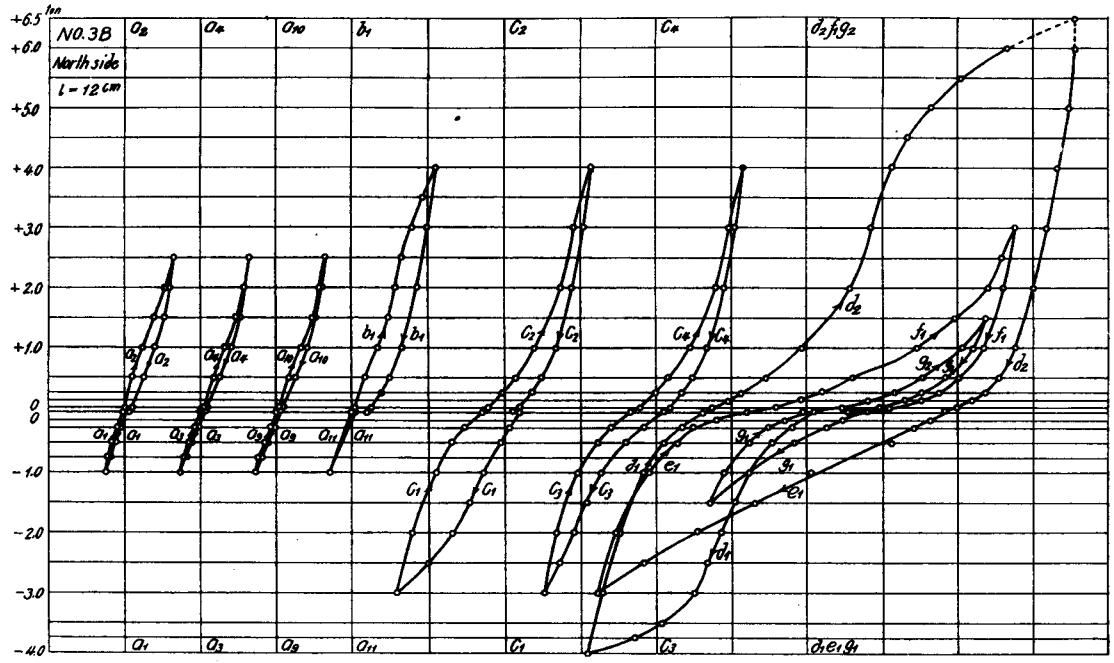

Graph. 9 (*Bs*)

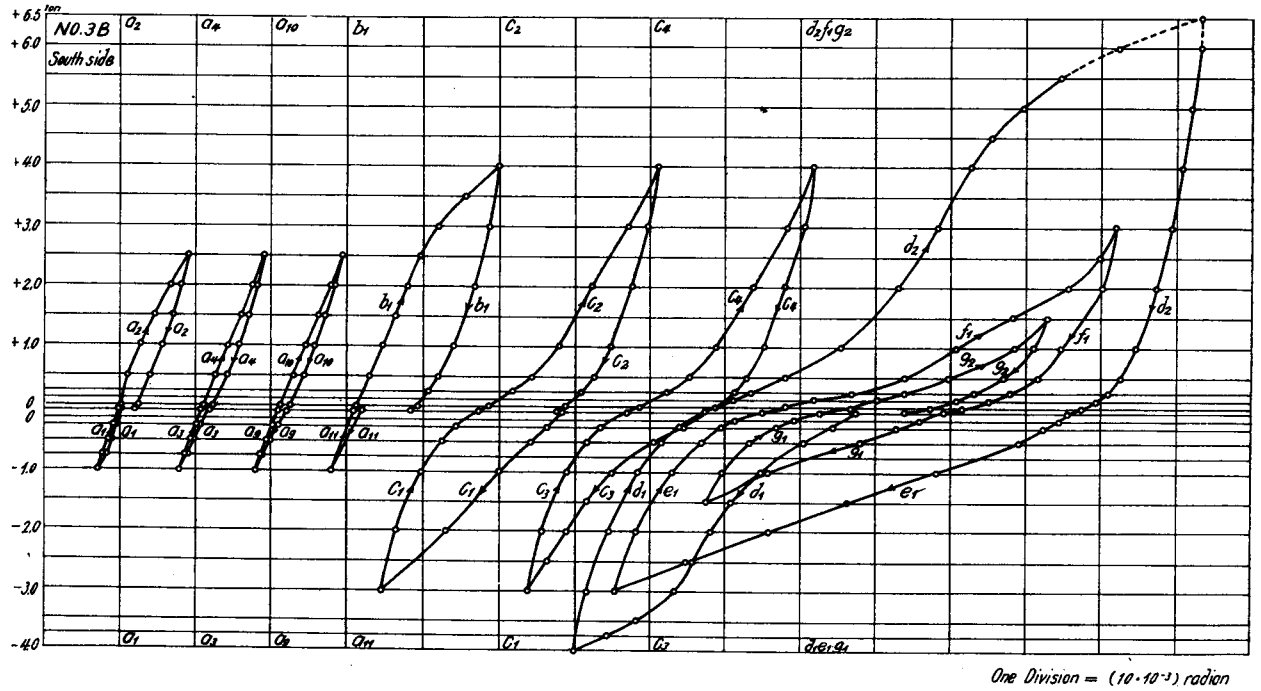

Graphs. 8, 9. Results for Test Piece No. 3.

Graph. 10.

Graph. 10 (*An*)

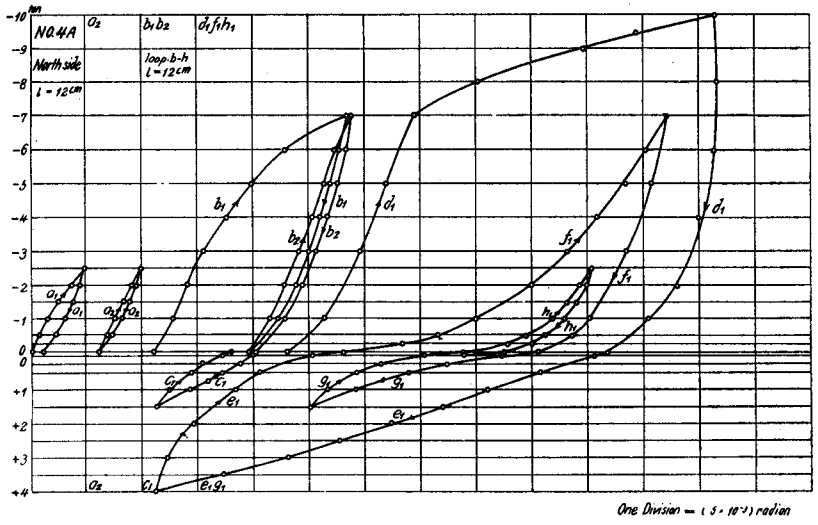

Graph. 10 (*As*)

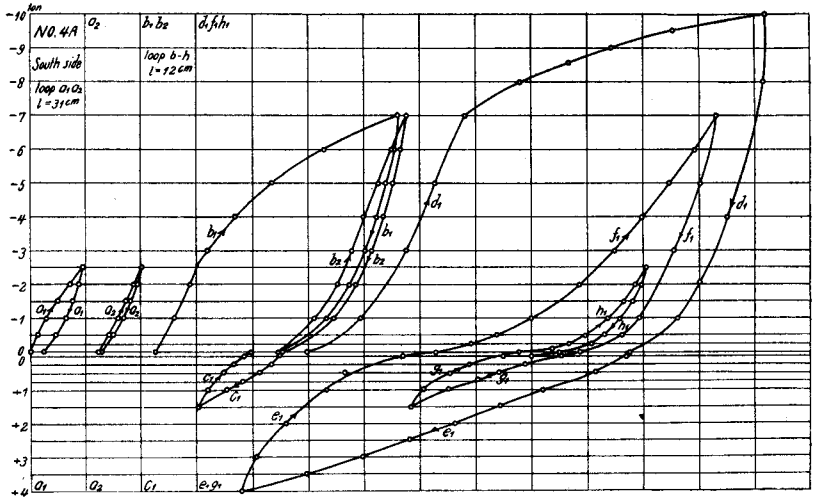

Graph. 11.

Graph. 11 (*Bn*)

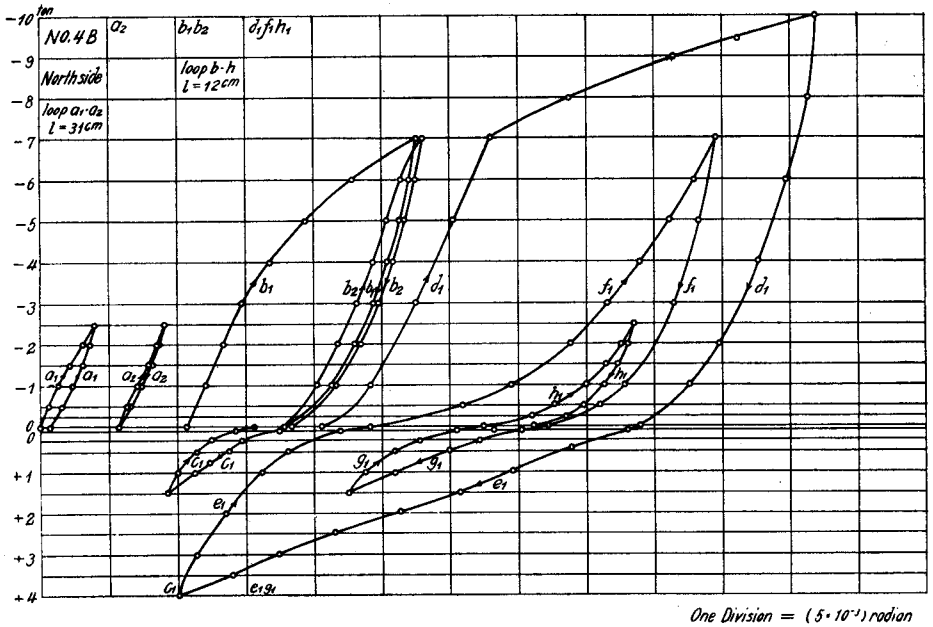

Graph. 11 (*Bs*)

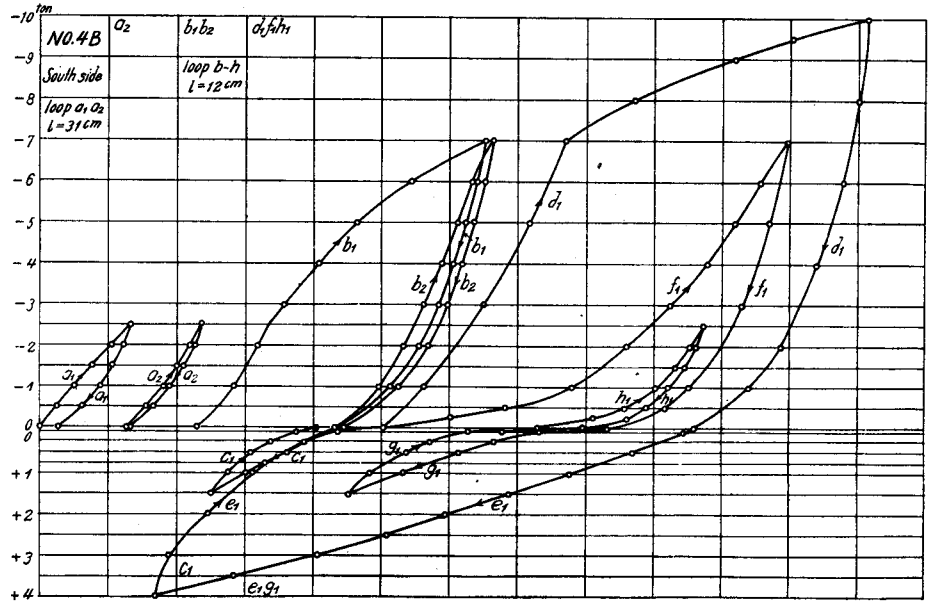

Graphs. 10, 11. Results for Test Piece No. 4.

Graph. 12.

Graph. 12 (*An*)

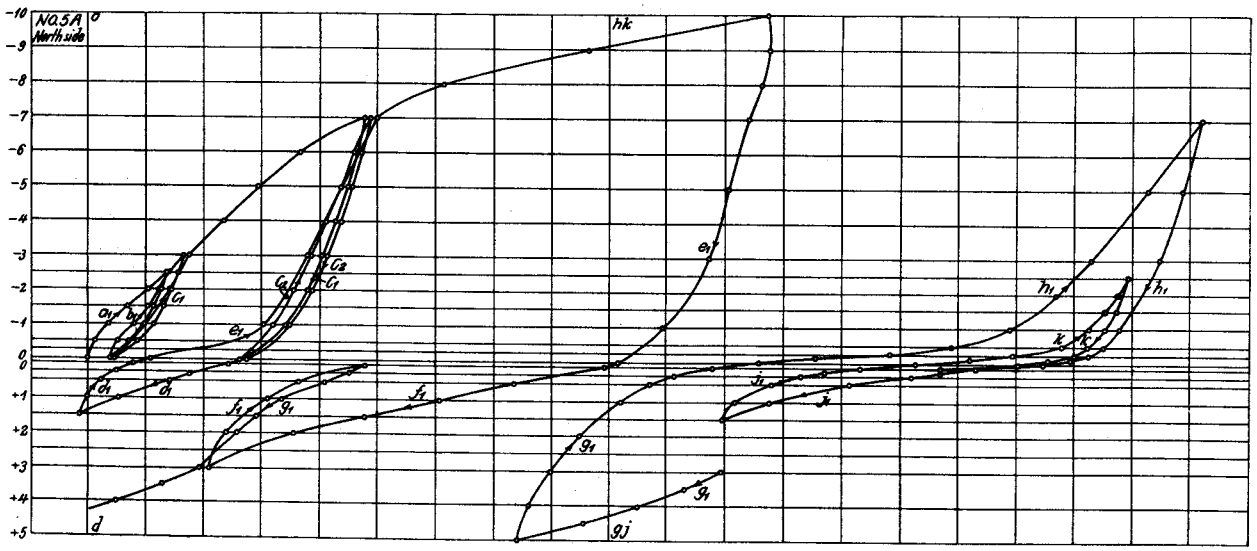

Graph. 12 (*As*)

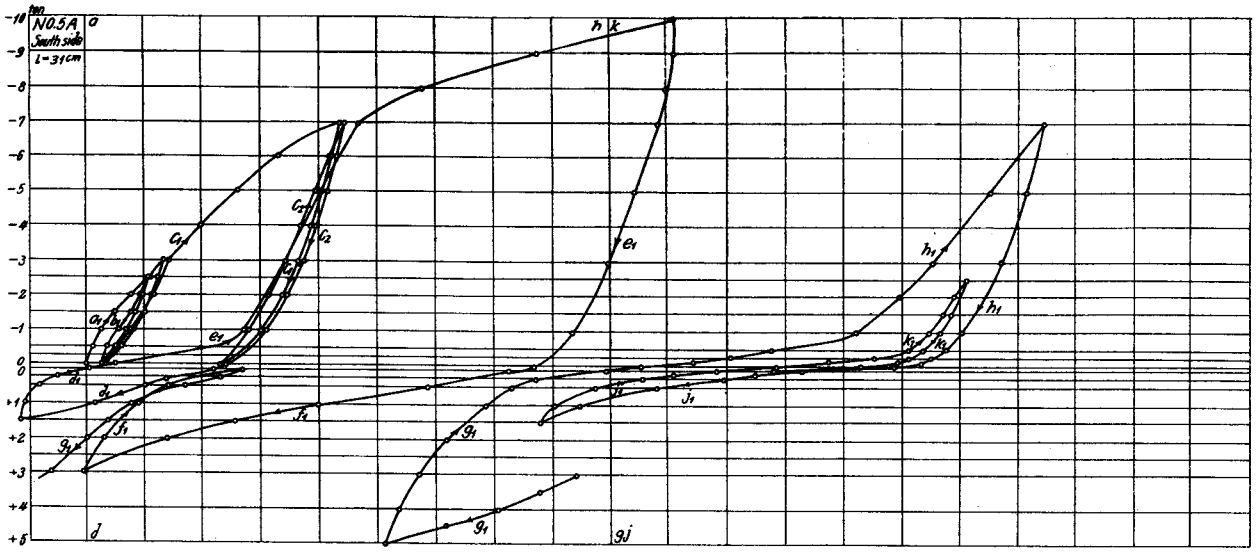

Graph. 13.

Graph. 13 (*Bs*)

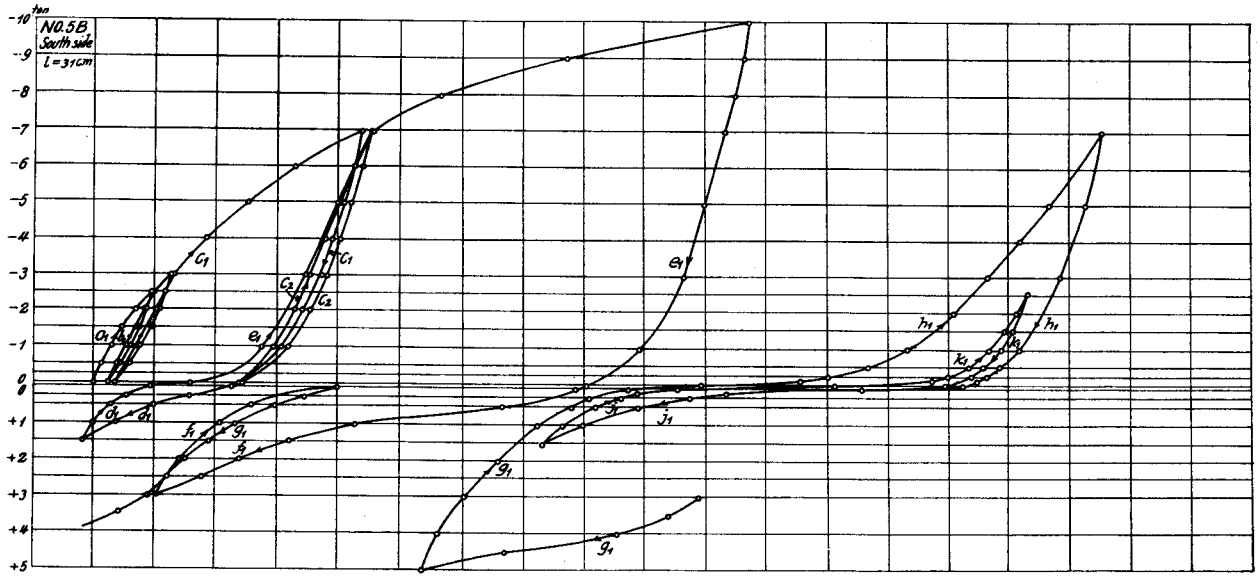

Graph. 13.

Graph. 13 (*Bn*)

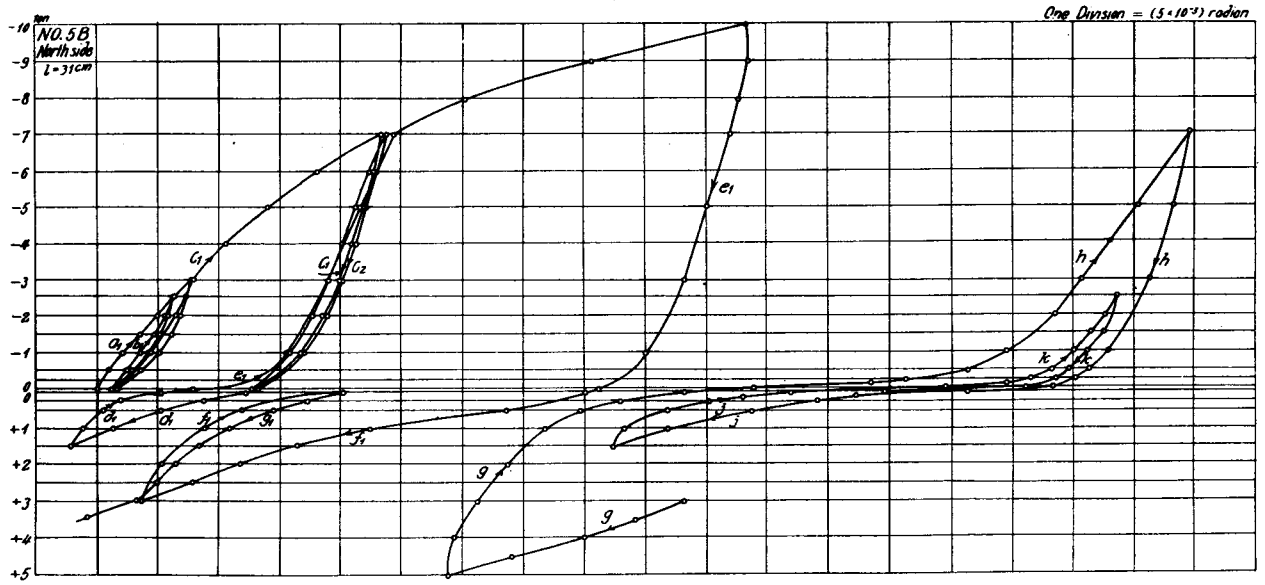

Graphs. 12, 13. Results Test Piece No. 5.

Graph. 14.

Graph. 14 (*As*)

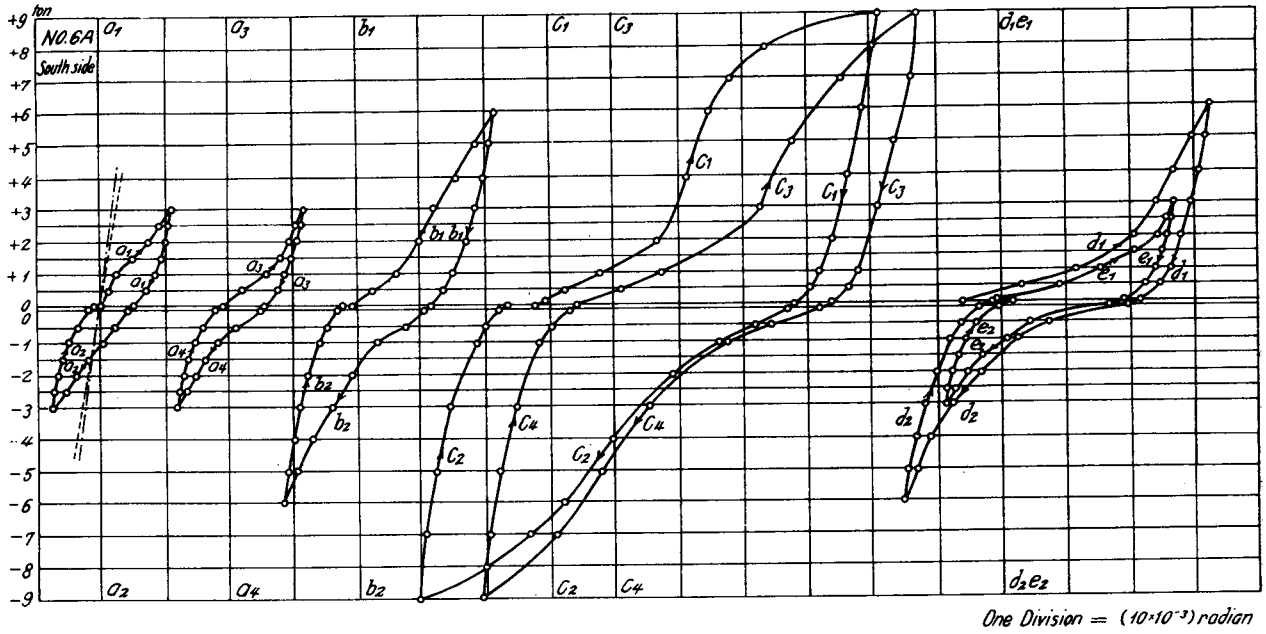

Graph. 14 (*An*)

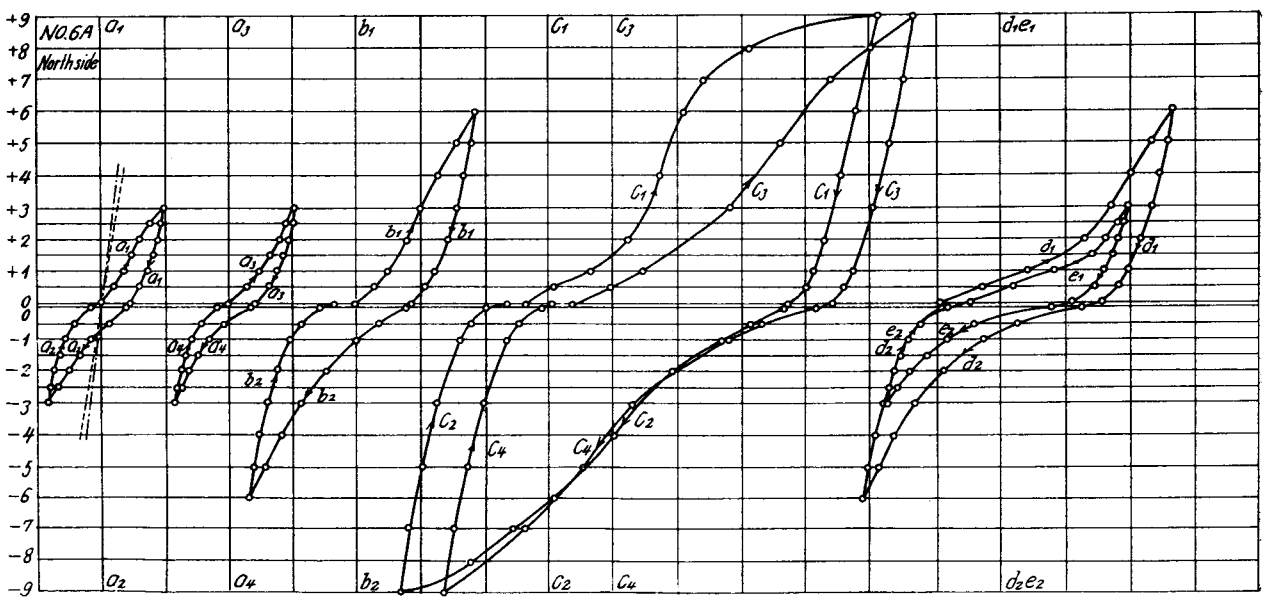

Graph. 15.

Graph. 15 (*Bs*)

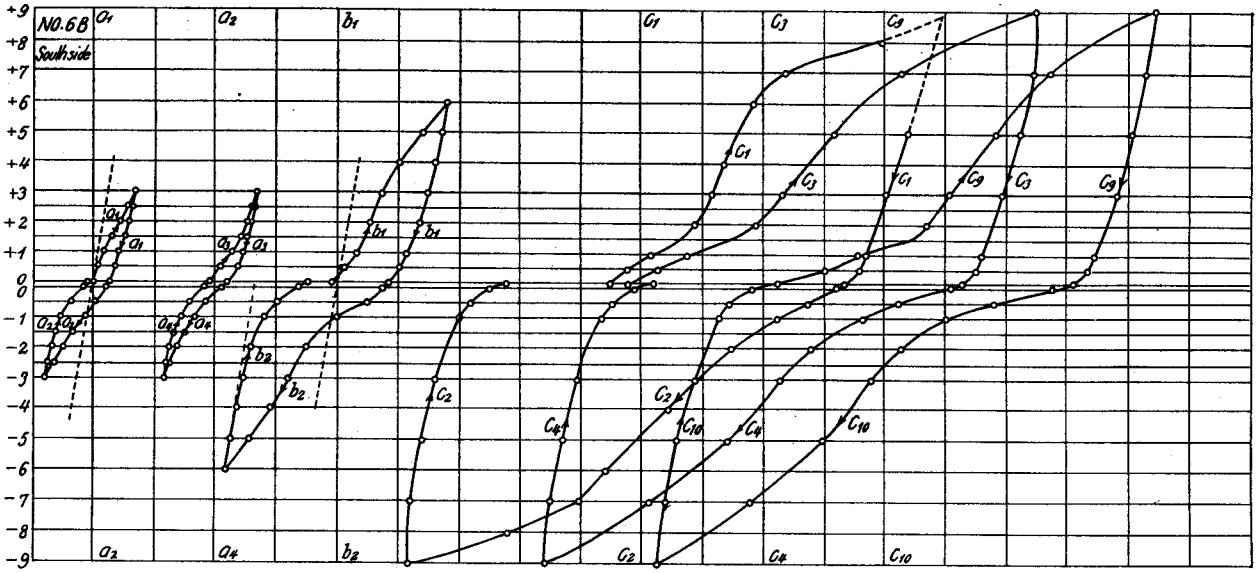

Graph. 15 (*Bn*)

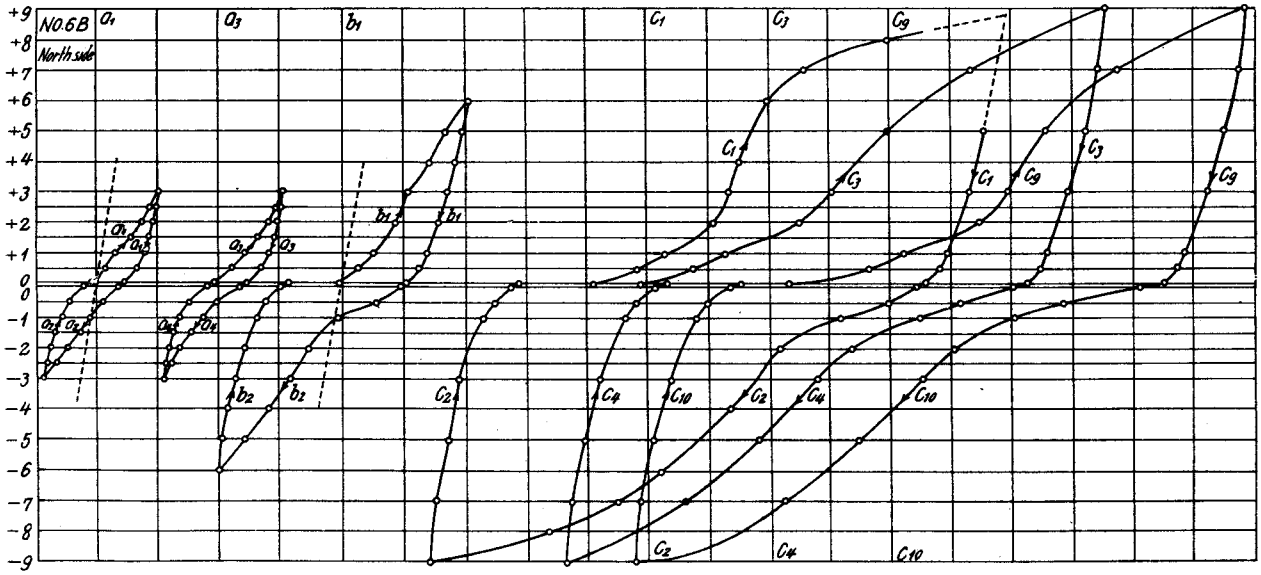

One Division = $(10 \cdot 10^{-3})$ radian

Graph. 15 (*Bs, n*)

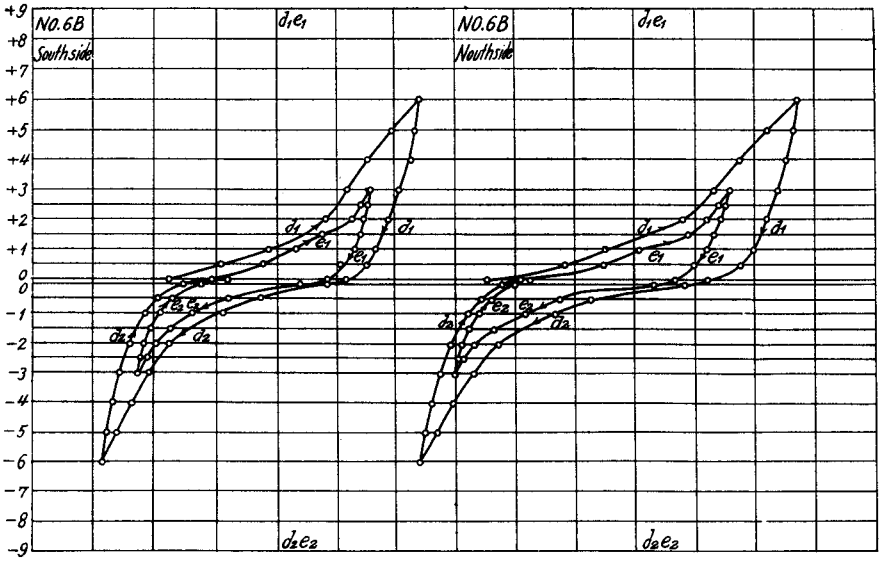

One Division = $(10 \cdot 10^{-3})$ radian

Graphs. 14, 15. Results for Test Piece No. 6.

Graph. 16 (*As, n*)

Graph. 16.

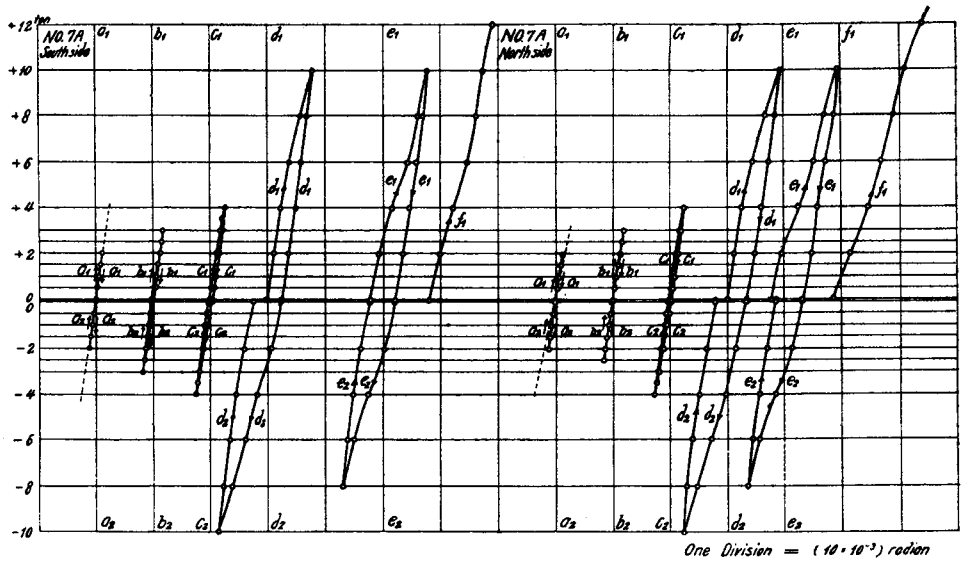

Graph. 17.

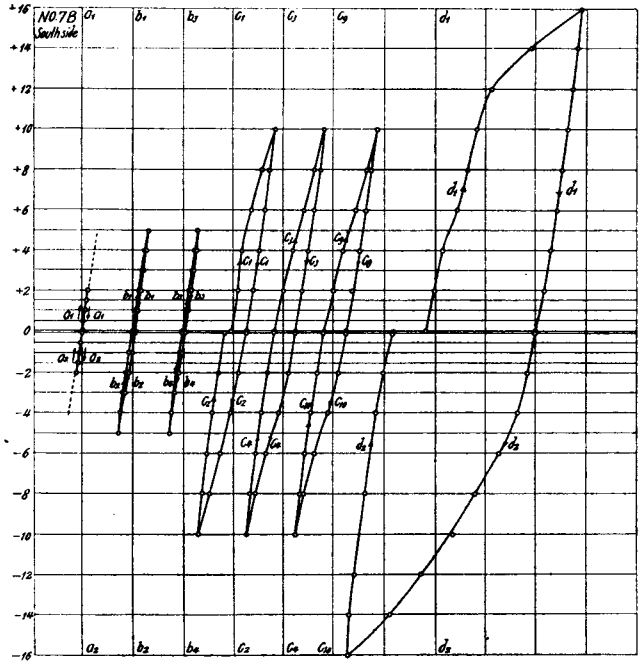

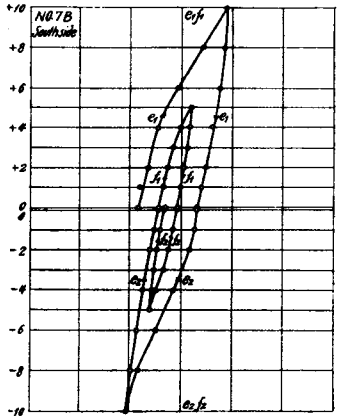

Graphs. 16, 17. Results for Test Piece No. 7.

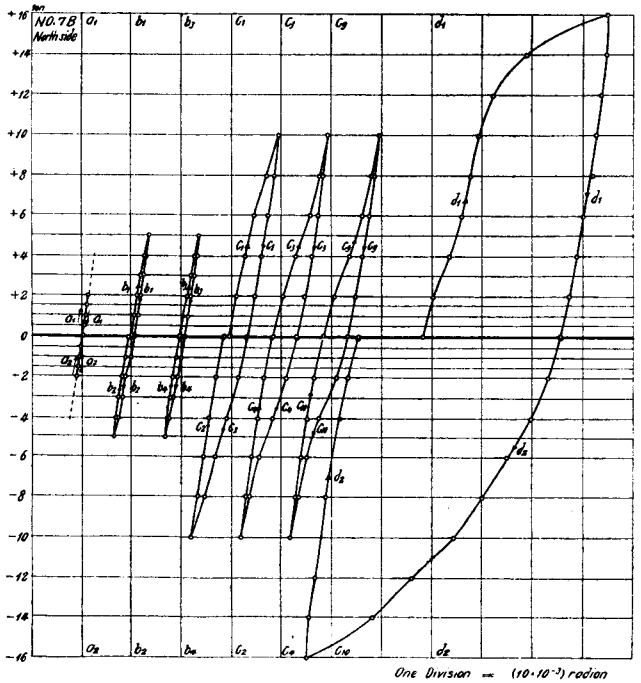

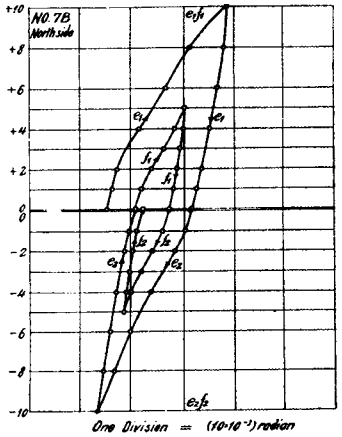

Graph. 18.

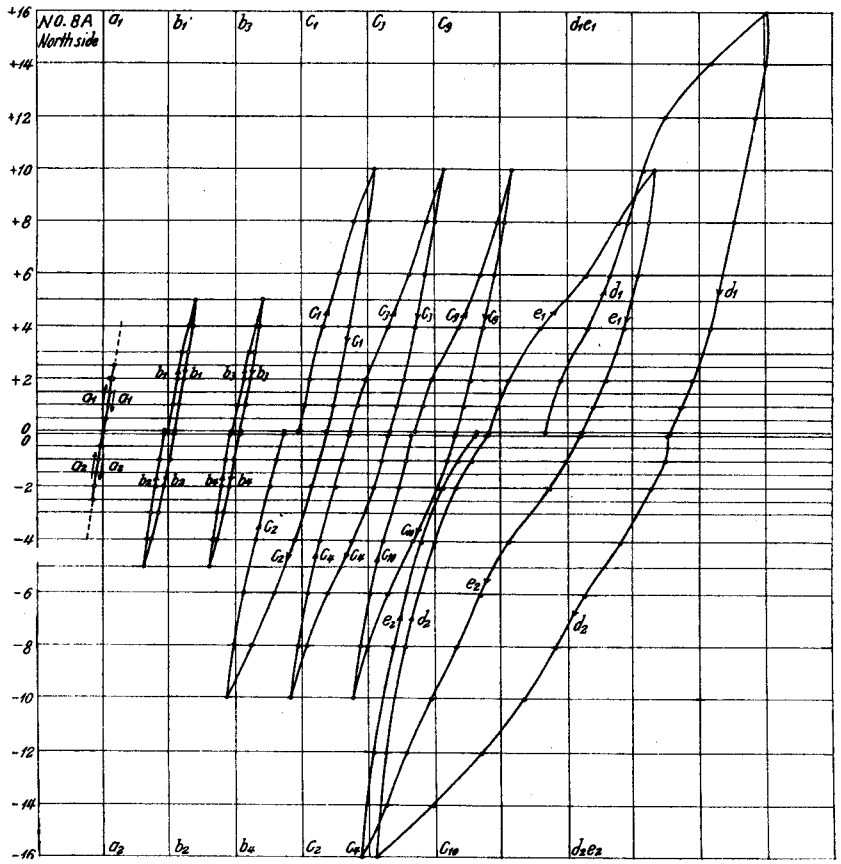
NO. 8A
North side
+16
+14
+12
+10
+8
+6
+4
+2
0
-2
-4
-6
-8
-10
-12
-14
-16

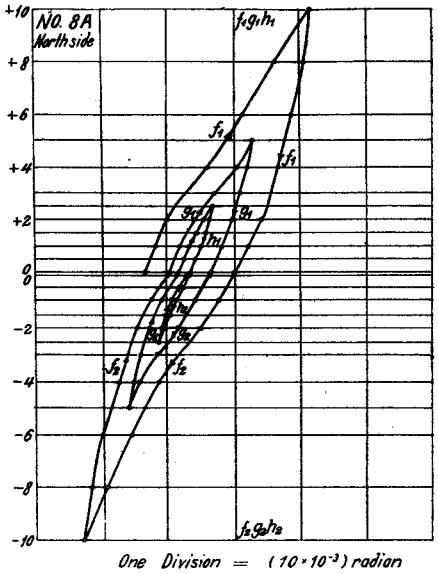
NO. 8A
North side
+10
+8
+6
+4
+2
0
-2
-4
-6
-8
-10
One Division = (10 × 10⁻³) radian

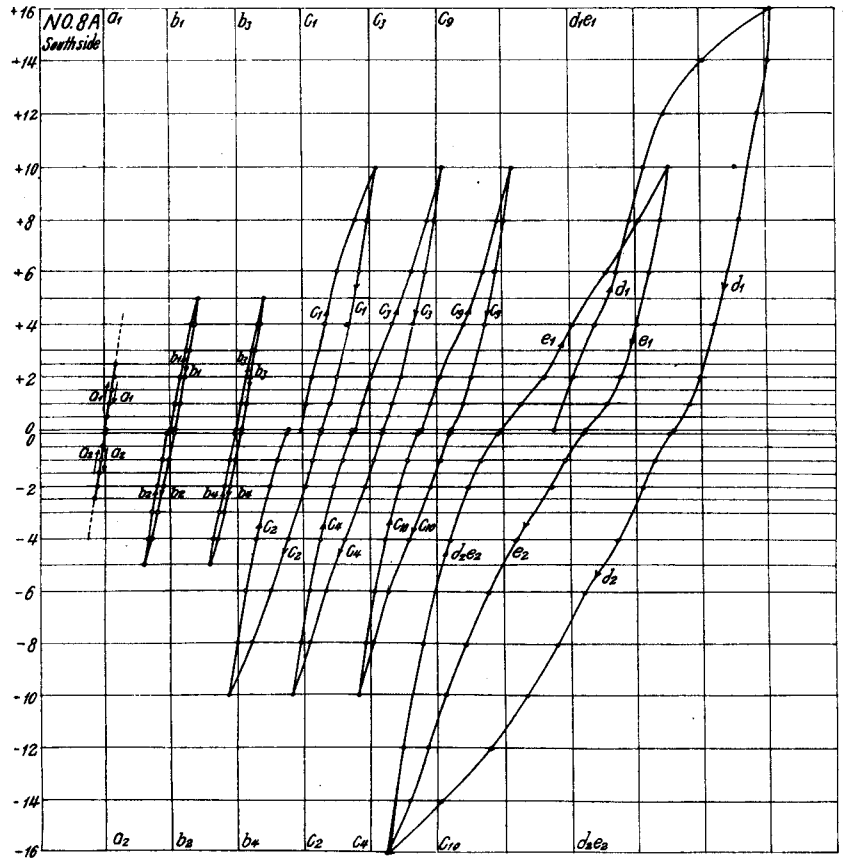
NO. 8A
South side
+16
+14
+12
+10
+8
+6
+4
+2
0
-2
-4
-6
-8
-10
-12
-14
-16

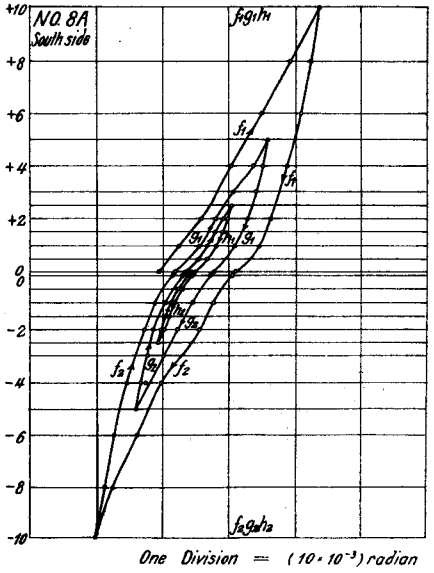
NO. 8A
South side
+10
+8
+6
+4
+2
0
-2
-4
-6
-8
-10
One Division = (10 × 10⁻³) radian

Graph. 19.

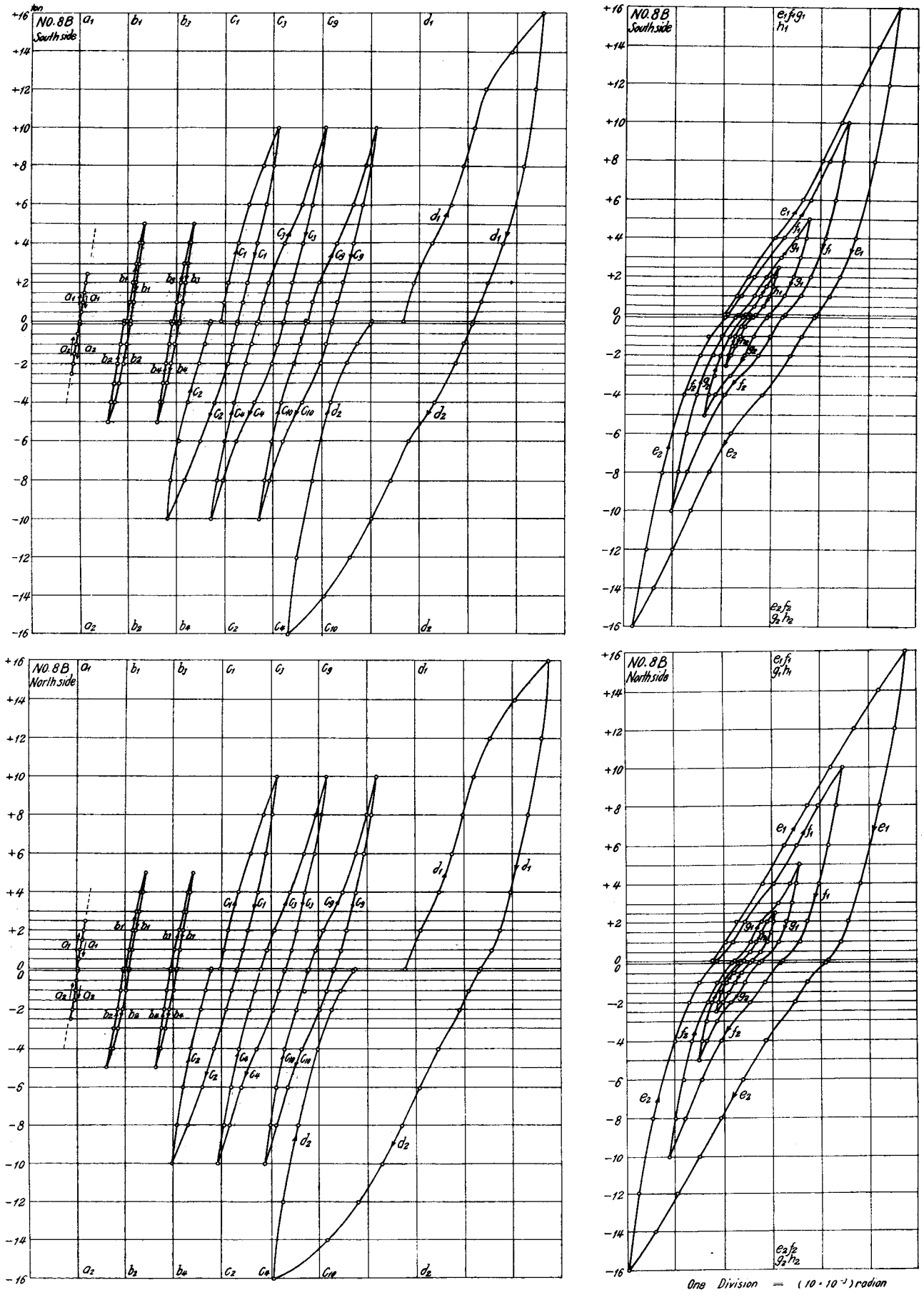

Graphs. 18, 19. Results for Test Piece No. 8.

Graph. 20.

Graph. 20 (*An*)

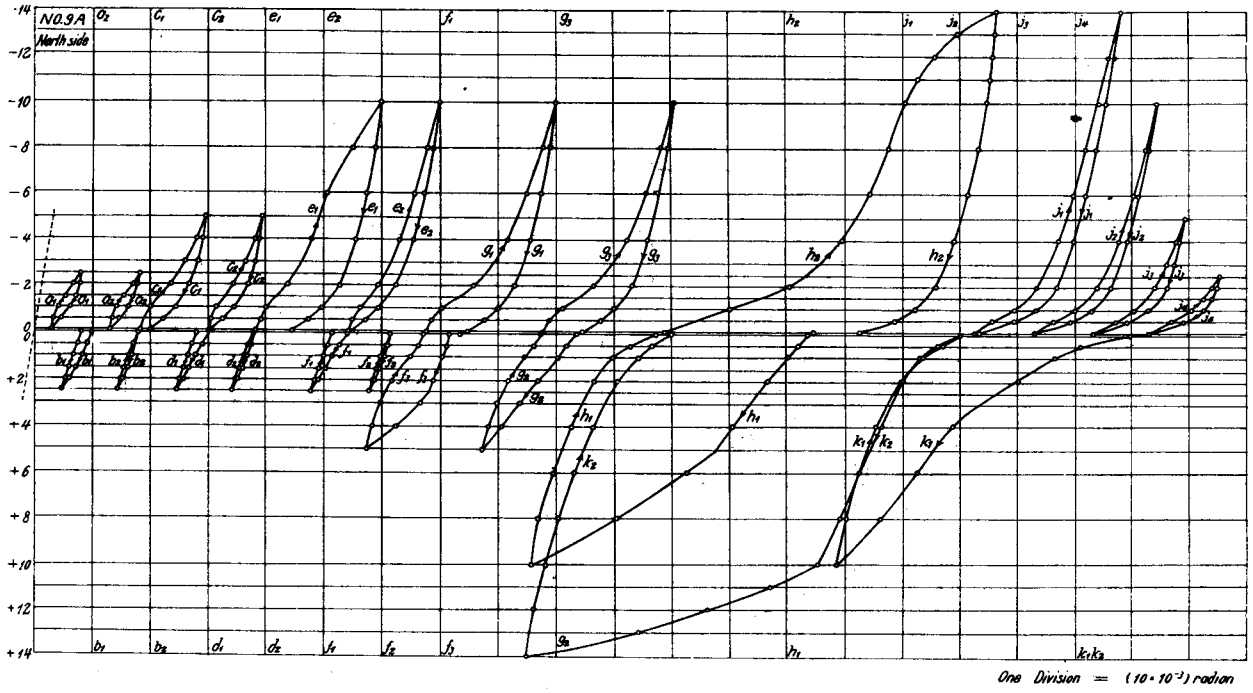

Graph. 20 (*As*)

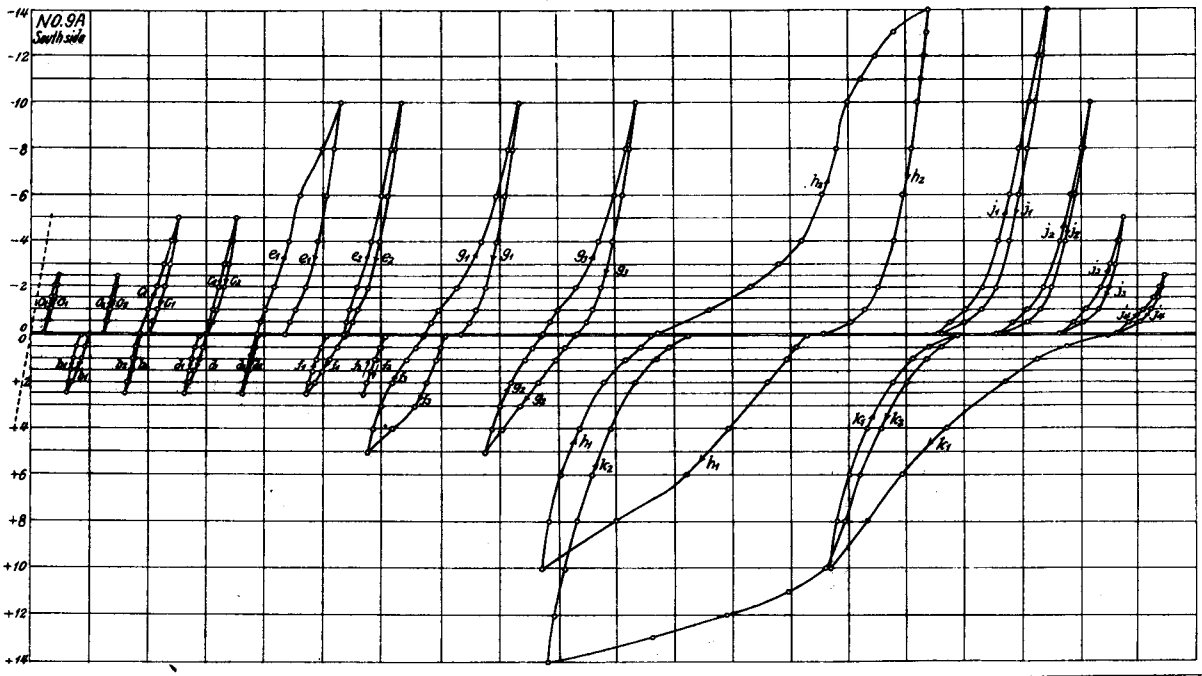

Graph. 20 (*As, n*)

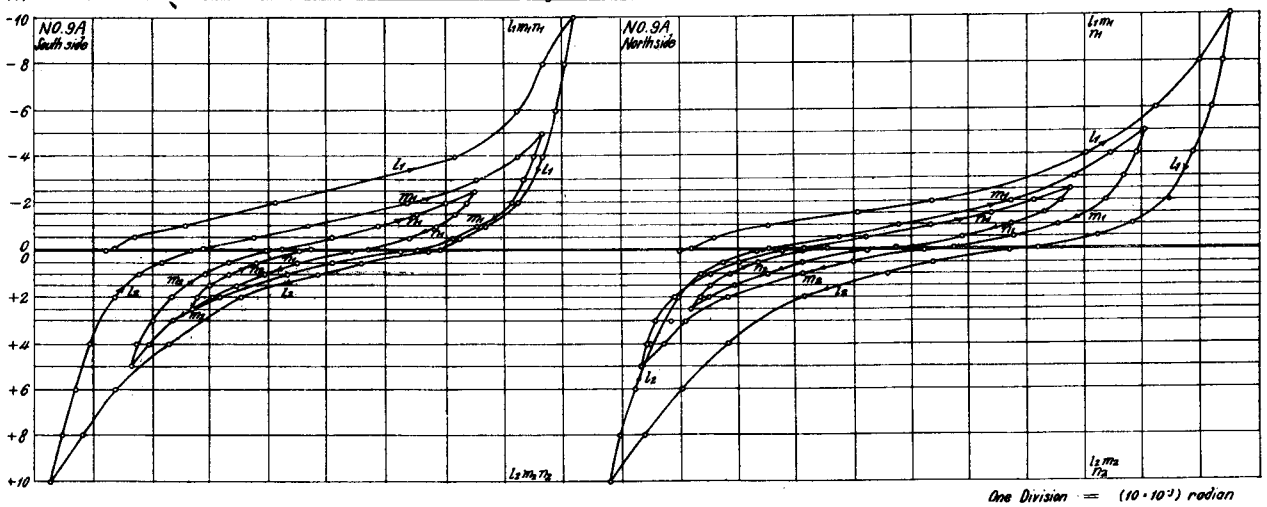

Graph. 20. Results for Test Piece No. 9.

Graph. 21.

Graph. 21 (*Bs*)

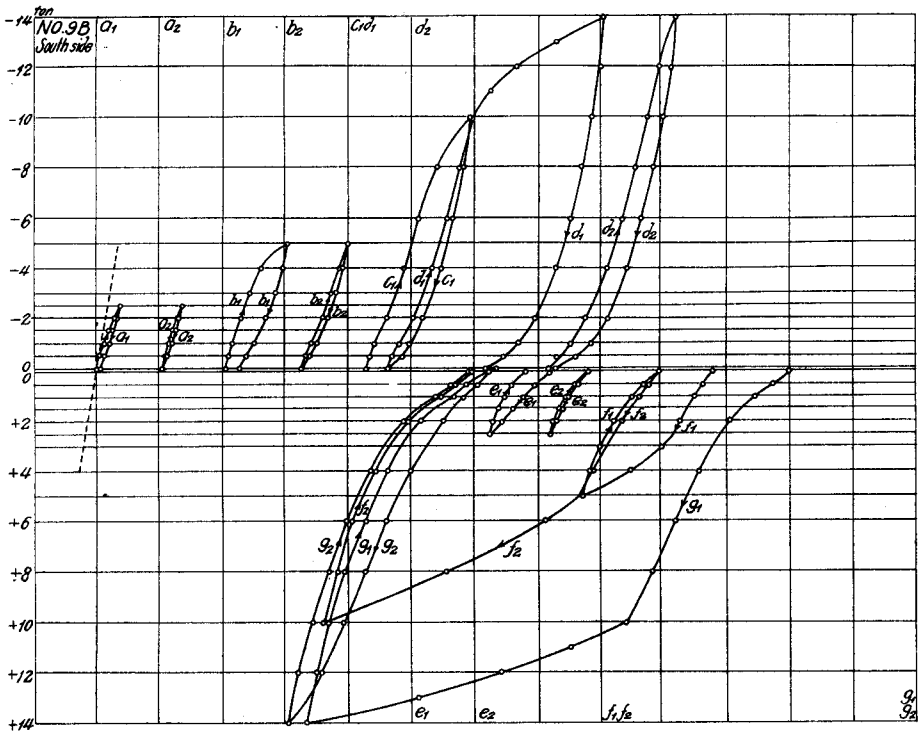

Graph. 21 (*Bn*)

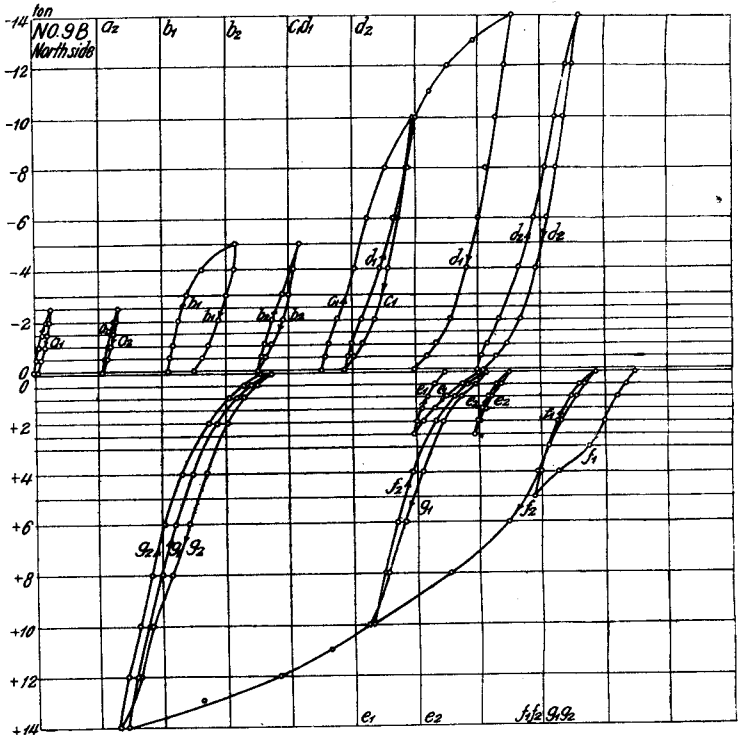

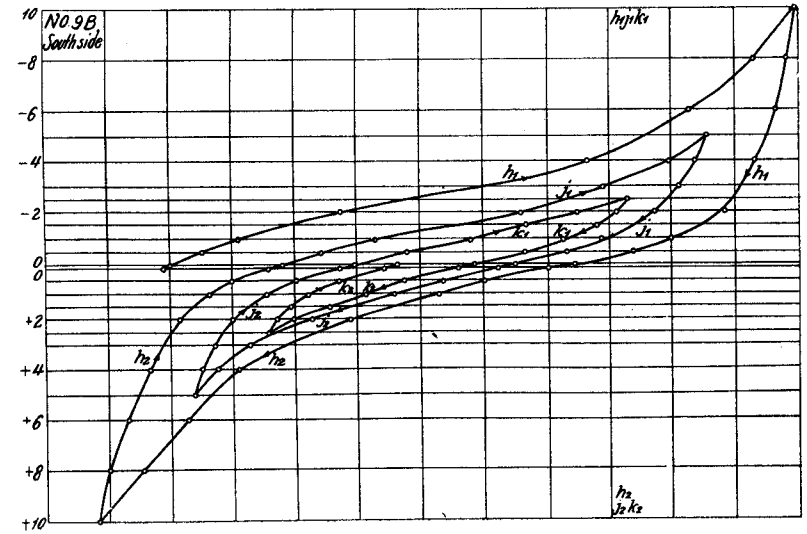

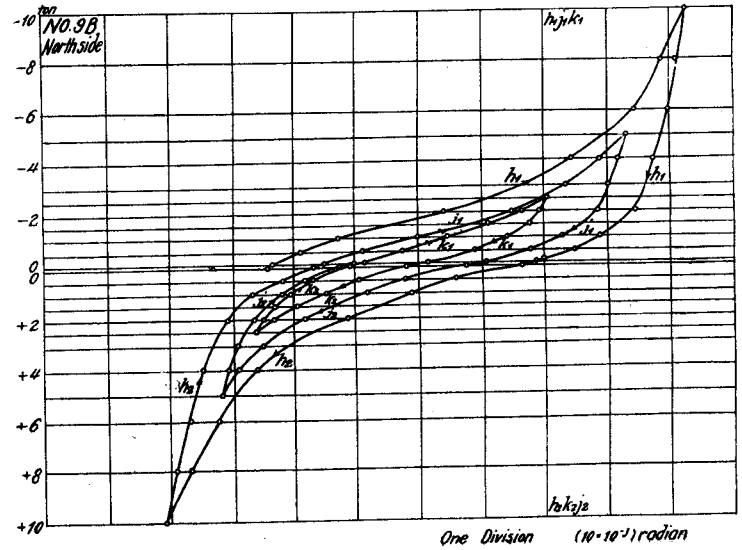

Graphs. 20, 21. Results for Test Piece No. 9.